NAVAL POSTGRADUATE SCHOOL

MONTEREY, CALIFORNIA

THESIS

PERFORMANCE COMPARISON OF FEDERAL AVIATION ADMINISTRATION RADARS AGAINST MULTIPLE AIRCRAFT TYPES

by

Benjamin A. Brannum

September 2023

Thesis Advisor: Ric Romero
Co-Advisor: David C. Jenn

This project was funded in part by the NPS Naval Research Program.

THIS PAGE INTENTIONALLY LEFT BLANK

REPORT DOCUMENTATION PAGE	*Form Approved OMB No. 0704-0188*

Public reporting burden for this collection of information is estimated to average 1 hour per response, including the time for reviewing instruction, searching existing data sources, gathering and maintaining the data needed, and completing and reviewing the collection of information. Send comments regarding this burden estimate or any other aspect of this collection of information, including suggestions for reducing this burden, to Washington headquarters Services, Directorate for Information Operations and Reports, 1215 Jefferson Davis Highway, Suite 1204, Arlington, VA 22202-4302, and to the Office of Management and Budget, Paperwork Reduction Project (0704-0188) Washington, DC, 20503.

1. AGENCY USE ONLY *(Leave blank)*	**2. REPORT DATE** September 2023	**3. REPORT TYPE AND DATES COVERED** Master's thesis

4. TITLE AND SUBTITLE
PERFORMANCE COMPARISON OF FEDERAL AVIATION ADMINISTRATION RADARS AGAINST MULTIPLE AIRCRAFT TYPES

5. FUNDING NUMBERS
NPS-23-N158-A

6. AUTHOR(S) Benjamin A. Brannum

7. PERFORMING ORGANIZATION NAME(S) AND ADDRESS(ES)
Naval Postgraduate School
Monterey, CA 93943-5000

8. PERFORMING ORGANIZATION REPORT NUMBER

9. SPONSORING / MONITORING AGENCY NAME(S) AND ADDRESS(ES)
N/A

10. SPONSORING / MONITORING AGENCY REPORT NUMBER

11. SUPPLEMENTARY NOTES The views expressed in this thesis are those of the author and do not reflect the official policy or position of the Department of Defense or the U.S. Government. This project was funded in part by the NPS Naval Research Program.

12a. DISTRIBUTION / AVAILABILITY STATEMENT
Approved for public release. Distribution is unlimited.

12b. DISTRIBUTION CODE
A

13. ABSTRACT (maximum 200 words)

The detection and tracking of aircraft and weather patterns are vital to the safety and success of the aviation industry both in the United States and throughout the world. In order to preserve and maintain situational awareness of the skies, the Federal Aviation Administration (FAA) employs four unique rotating radar systems: Air Surveillance Radar 9 (ASR-9), Air Surveillance Radar 11 (ASR-11), Terminal Doppler Weather Radar (TDWR), and Air Route Surveillance Radar (ARSR-4). In this work, an analysis of extending the capabilities of these radars is completed by allowing coherent processing of the maximum number of returned pulses within the antenna beamwidth. This analysis is performed by developing a Matrix Laboratory (Matlab) code set as a means through which a comprehensive comparison can be made. This research compares each radar target detection capability across multiple parametric studies with signal-to-noise ratio (SNR), target radar cross section (RCS), and Doppler frequency. Output results of this analysis also include two-dimensional beam comparisons of each radar against varying sized targets. The analysis features multiple aircraft SNR vs. range, range vs. RCS, beam comparisons, and Doppler frequency comparisons with both a single pulse transmission and the maximum possible number of pulses within the antenna beamwidth.

14. SUBJECT TERMS
radar, rotating radar, detection, range, FAA, Federal Aviation Administration, signal-to-noise ratio, SNR, target radar cross section, RCS, ASR-9, ASR-11, TDWR, ARSR-4, Air Surveillance Radar, Terminal Doppler Weather Radar, Air Route Surveillance Radar

15. NUMBER OF PAGES
85

16. PRICE CODE

17. SECURITY CLASSIFICATION OF REPORT	**18. SECURITY CLASSIFICATION OF THIS PAGE**	**19. SECURITY CLASSIFICATION OF ABSTRACT**	**20. LIMITATION OF ABSTRACT**
Unclassified	Unclassified	Unclassified	UU

NSN 7540-01-280-5500

Standard Form 298 (Rev. 2-89)
Prescribed by ANSI Std. 239-18

THIS PAGE INTENTIONALLY LEFT BLANK

Approved for public release. Distribution is unlimited.

PERFORMANCE COMPARISON OF FEDERAL AVIATION ADMINISTRATION RADARS AGAINST MULTIPLE AIRCRAFT TYPES

Benjamin A. Brannum
Captain, United States Marine Corps
BSME, University of Tennessee, Knoxville, 2017

Submitted in partial fulfillment of the
requirements for the degree of

MASTER OF SCIENCE IN ELECTRICAL ENGINEERING

from the

NAVAL POSTGRADUATE SCHOOL
September 2023

Approved by: Ric Romero
Advisor

David C. Jenn
Co-Advisor

Douglas J. Fouts
Chair, Department of Electrical and Computer Engineering

THIS PAGE INTENTIONALLY LEFT BLANK

ABSTRACT

The detection and tracking of aircraft and weather patterns are vital to the safety and success of the aviation industry both in the United States and throughout the world. In order to preserve and maintain situational awareness of the skies, the Federal Aviation Administration (FAA) employs four unique rotating radar systems: Air Surveillance Radar 9 (ASR-9), Air Surveillance Radar 11 (ASR-11), Terminal Doppler Weather Radar (TDWR), and Air Route Surveillance Radar (ARSR-4). In this work, an analysis of extending the capabilities of these radars is completed by allowing coherent processing of the maximum number of returned pulses within the antenna beamwidth. This analysis is performed by developing a Matrix Laboratory (Matlab) code set as a means through which a comprehensive comparison can be made. This research compares each radar target detection capability across multiple parametric studies with signal-to-noise ratio (SNR), target radar cross section (RCS), and Doppler frequency. Output results of this analysis also include two-dimensional beam comparisons of each radar against varying sized targets. The analysis features multiple aircraft SNR vs. range, range vs. RCS, beam comparisons, and Doppler frequency comparisons with both a single pulse transmission and the maximum possible number of pulses within the antenna beamwidth.

THIS PAGE INTENTIONALLY LEFT BLANK

Table of Contents

List of Figures

List of Tables

THIS PAGE INTENTIONALLY LEFT BLANK

List of Acronyms and Abbreviations

A310	Airbus A310
ARSR-3	Air Route Surveillance Radar 3
ARSR-4	Air Route Surveillance Radar 4
ASR-7	Air Surveillance Radar 7
ASR-8	Air Surveillance Radar 8
ASR-9	Air Surveillance Radar 9
ASR-11	Air Surveillance Radar 11
CN-235	Construcciones Aeronáuticas SA CN-235
DHS	Department of Homeland Security
DOD	Department of Defense
F-16	Lockheed Martin F-16 Fighting Falcon
FAA	Federal Aviation Administration
GPS	Global Positioning System
HPBW	half-power beamwidth
Matlab	Matrix Laboratory
MIT	Massachusetts Institute of Technology
NEXRAD	Next Generation Radar
NOAA	National Oceanographic and Atmospheric Administration
PRF	pulse repetition frequency

RCS	radar cross section
RRE	radar range equation
SNR	signal-to-noise ratio
TDWR	Terminal Doppler Weather Radar
TTA	time to arrival

Acknowledgments

I'd like to take this opportunity to thank my wife, Sydney, for her unwavering support and encouragement. To my parents, Terry and Amy, thank you for always supporting me in everything I pursue. Thanks to my siblings, Ellie, Nick, and John, for being there for me. Last, but certainly not least, my advisors Professor Romero and Professor Jenn for guidance and knowledge throughout the research process.

THIS PAGE INTENTIONALLY LEFT BLANK

CHAPTER 1:
Introduction

1.1 Motivation

Maintaining accurate locations of in-transit aircraft is important in the aviation industry. With over sixteen million flights and forty-four billion pounds of freight transported via air each year, preventing mishaps is no small task [1]. In addition to civilian use, the military also performs a significant number of flights for the movement of personnel and equipment each year. While the Department of Defense (DOD) operates worldwide, most domestic flights are subject to Federal Aviation Administration (FAA) guidelines and communication requirements. It is necessary for aviation units in the DOD to understand how their aircraft are detected by the FAA radar systems and at what range the detection is anticipated. Lastly, but most certainly not least, a key aspect of national defense is the identification of aircraft attempting to enter U.S. controlled airspace. While many of these encounters are from international arrivals, the U.S. must be prepared for adversary incursions in the form of military targets or illicit, black-market transportation. The FAA, DOD, and Department of Homeland Security (DHS) have a vested interest in ensuring deconfliction between civilian and military flights in order to facilitate safe and efficient use of airspace.

While the modern Global Positioning System (GPS) provides the ability to precisely determine the location of aircraft, it is necessary to have additional means to locate aircraft from the ground in the event of interference, malfunction, or failure. The FAA employs four radar systems enable reliable and redundant aircraft detection within U.S. airspace, bolstering the ability to locate aircraft while in flight and maintain constant awareness. Additionally, the FAA radars possess varying degrees of weather tracking ability, however, the weather-related radar aspect is not the focus of the research. The focus of this study is detection performance analysis and comparison of these radars solely emphasizing various target aircraft. There is additional benefit to investigate potential upgrade to a coherent receiver system to improve radar performance.

The given detection ranges for each radar system in the specification sheets provide a singular

radar cross section (RCS) value, usually 1 m^2, which is later shown in Table 2.1. It also includes one weather tracking sensitivity value in dBZ. This research serves as a basis for further investigation into FAA radar detection performance against multiple aircraft types and the resulting detection ranges. Thus, practically in this thesis work, the target parameter of interest is RCS and not reflectivity Z. This thesis proposes to accomplish this goal in two ways: a) use of maximum number of pulses returned in antenna beamwidth and b) coherent receiver detection. Of course, these propositions can also help FAA radar receiver modernization towards system updates since these radars were designed and implemented in the 1990s.

1.2 Objectives

The objective in this thesis is to provide a performance comparison of the four FAA radar systems, Air Surveillance Radar 9 (ASR-9), Air Surveillance Radar 11 (ASR-11), Terminal Doppler Weather Radar (TDWR), and Air Route Surveillance Radar 4 (ARSR-4), regarding their ability to detect three different aircraft of varying size, or in this case, RCS effective area. Initially using one transmission pulse, comparisons of received signal-to-noise ratio (SNR) as a function of target range from the radar are also presented to evaluate system performance. To aid in the development of results, Matrix Laboratory (Matlab) is used to develop a code set that parameterizes the necessary input data to generate the following output performance curves: SNR vs. target range, target range vs. RCS, and Doppler frequency vs. target velocity. Additionally, a radar beam plot is generated with the axes in horizontal distance and vertical altitude, which compares both the antenna beam shapes and detection ranges. The beams are annotated with the center beam detection range as well as the half-power beamwidth (HPBW) detection range. The remainder of the performance results comparison utilizes the theoretical maximum number of possible pulses as a function of rotation rate and azimuth beamwidth. Recall it is proposed to use maximum number of pulses to each radar to extend its performance.

1.3 Related Work

Although the work in this thesis develops an implementation of a Matlab-based radar system performance and detection capability comparison, there is some existing related research in the field of FAA radar systems and target aircraft detection. The first work [2] investigated the

radar systems used by the FAA. This research focused on the development of requirements for a future multi-function, phased array radar system to either complement or replace the current FAA radar systems [2].

Additionally, the work in [3] investigated a possible case to bolster the National Oceanographic and Atmospheric Administration (NOAA) weather radar network. This document proposed how FAA radar systems could complement existing NOAA capabilities and how this interconnectivity between radar networks would significantly increase the weather tracking of each entity [3].

Finally, the work in [4] focused on unidentified radar target detection of varying RCS and velocity. In order to do this, a neural network design was proposed and implemented to determine the unknown target aircraft velocity [4]. Different aircraft RCS and velocity values were used to expand the results to multiple aircraft types and sizes. This approach was used in order to evaluate system performance against a variety of aircraft.

1.4 Organization

This thesis is organized into five chapters. Chapter 2 provides a brief background in radar detection to provide foundational knowledge for the subsequent chapters. Chapter 2 also contains a brief overview of each radar system and aircraft used in the analysis. Chapter 3 discusses the overall methodology of the radar comparison study, as well as the assumptions and constraints imposed within the Matlab code. Chapter 4 presents performance results in terms of SNR vs. range, radar beam comparisons, range vs. RCS, and Doppler frequency for all three aircraft with additional tables containing a radar comparison summary. Results are organized into performance comparison using a single pulse transmission and transmission using the maximum number of pulses in a single beamwidth. The summary tables contain both center beam and HPBW detection ranges with their corresponding time to arrival (TTA) values from each aircraft. In Chapter 5, conclusions are drawn from the preceding chapters and offers suggestions and ideas for future work in this area of study.

THIS PAGE INTENTIONALLY LEFT BLANK

CHAPTER 2:
Background

2.1 Rotating Radar Fundamentals

Rotating radar systems, specifically airport radars, use rotating antennas to detect the position, range, and / or velocity of various aircraft. The rotating antenna sends out a beam of radio wave pulses, which bounce off the surface of the aircraft and return to the antenna. The antenna rotates at a fixed rate in the azimuth direction so that the beam scans a full 360° around the radar system. The radar measures the time it takes for the pulse waves to return at the bearing from which the return signal is received [5]. The radar system can then determine the distance to the aircraft. The change in frequency of the waves as they bounce off the aircraft can be used to determine its velocity radial to the radar or airport. The angular position of the radar antenna when the returning wave is received may also be used to determine the aircraft direction of travel [5]. The frequency of the radio waves used by a rotating radar system can vary depending on the application. Most contemporary, long-range radar systems operate between L and C band (1 – 8 GHz).

The rotating antenna of a radar system is usually mounted above the ground on a tower or mast. Radar systems are placed above ground level to reduce interference from buildings and trees and to provide a clear line-of-sight for the radar system. The speed of rotation of the antenna can also vary depending on the application. For example, air traffic control radar systems typically rotate faster than weather radar systems. This is because air traffic control radar systems need to scan a volume of space more quickly in order to detect all the aircraft in the area. This will also impact the rate at which a radar system will detect and / or track the same target again as it completes multiple rotations. If a radar is too slow, it will have a difficult time keeping track of the different targets it has detected. The radar system can be equipped with a variety of additional features, such as altimeters, transponders, and Doppler processing [5]. These features can be used to improve the accuracy and range of the radar system.

Transponders are devices that are installed on aircraft and other objects. When a transponder

receives a radar signal, it sends back a signal that contains information about the object, such as its identification, altitude, and velocity. This information can be used to track the object and to identify it [4]. Doppler radar measures the change in frequency of the radio waves as they bounce off an object. Doppler radar can be used to determine the radial velocity of objects, even if they are not moving directly towards or away from the radar system [5]. Rotating radars are an essential tool for detecting and tracking the many aircraft traversing U.S. airspace at any given time.

2.2 FAA Radar Network and Specifications

The FAA operates and maintains an expansive network of rotating radars to successfully detect and track aircraft. In total, they operate over 400 radar systems, which is a mix of ASR-9, ASR-11, TDWR, and ARSR-4. A 2002 U.S. map containing radar locations is shown in Figure 2.1. This figure does not include, however, the locations of the DOD-owned and operated radar systems.

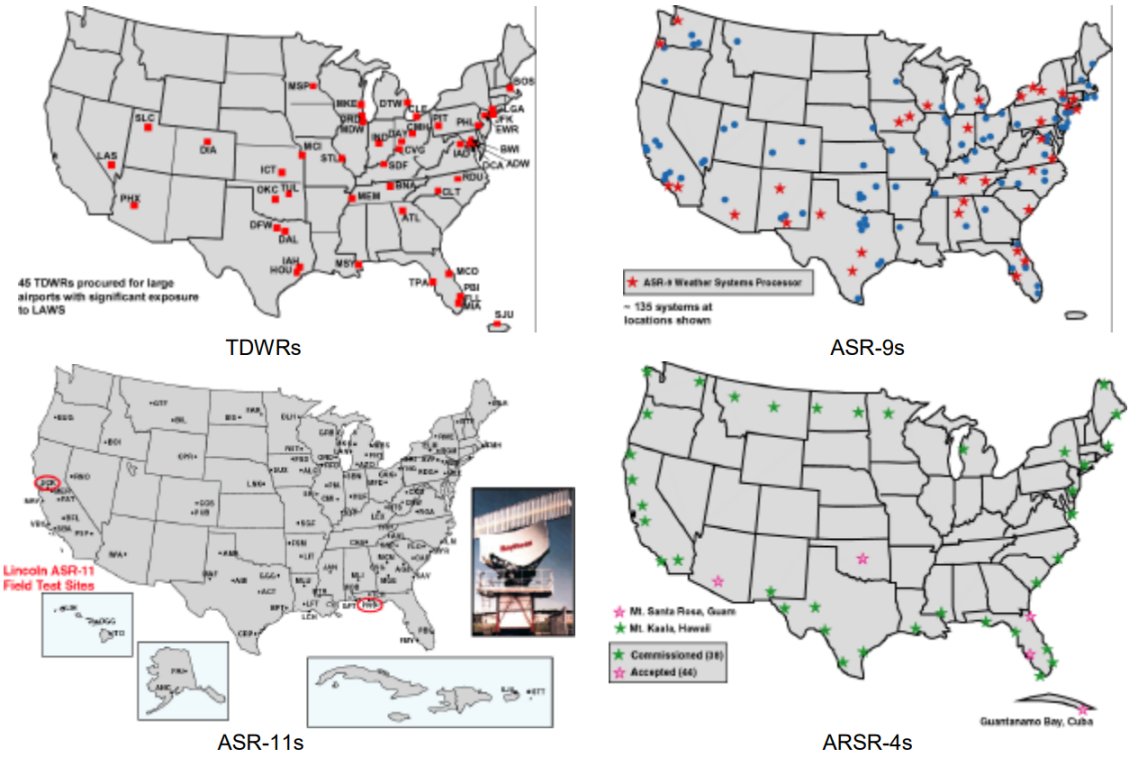

Figure 2.1. Locations of Federal Aviation Administration radar systems as of 2002. Source: [3].

As shown, the figure delineates between each radar type. It is interesting to note the locations of the ARSR-4 radars along the perimeter of the U.S. and one additional location at Guantanamo Bay, Cuba. This offers insight to the ability of the radar to detect aircraft at long range in order to maintain security of national airspace. Though comprehensive in nature, the data in this figure is somewhat outdated. An additional figure fills in any gaps left by [3]. Figure 2.2 shows all 513 radar systems in operation (excluding DOD), including the National Weather Service Next Generation Radar (NEXRAD) systems.

Figure 2.2. Locations of Federal Aviation Administration / Next Generation Radar systems as of 2015. Source: [6].

In addition to the radar system locations, another important aspect is the system specifications. Table 2.1 contains the most pertinent radar system specifications and provides a starting point for the radar performance comparisons performed in this research. Each radar mentioned will be further introduced and discussed in the next sections. Table 2.1 offers sensitivity in m^2 and dBZ. The unit dBZ is useful in meteorological applications, as it relates the radar reflectivity to the volume reflectivity of rain [5]. The dBZ scale helps relate radar reflectivity to approximate rainfall rates in weather mapping [5]. It was mentioned that the focus in this research is purely detection of aircraft and not weather-related targets. Again, in the study, the parameter to use is RCS. Indeed, in this thesis, weather factors are considered as additional noise or loss in SNR received, which will be accounted for in later chapters.

Table 2.1. Specifications for Federal Aviation Administration radar systems. Source: [3].

	TDWR (Raytheon)	ASR-9 (Northrop Grumman)	ASR-11 (Raytheon)	ARSR-4 (Northrop Grumman)
Transmitter				
Frequency	5.5 - 5.65 GHz ~ C Band	2.7-2.9 GHz	2.7-2.9 GHz	1.2-1.4 GHz
Polarization	Linear	Linear or Circular	Linear or Circular	Linear or Circular
Peak Power	250 KW	1.1 MW	20 kw	60 kw
Pulse Width	1.1 μs	1.0 μs	1.0 μs, 80 μs	150 μs
PRF	2000 (max)	2 CPIs (~ 1000 Hz avg.)	4 CPIs (~ 1000 Hz avg.)	9-pulse CPI at variable spacing (288 Hz avg)
Receiver				
Sensitivity	0 dBz @ 190 km 1 m^2 @ 460 km	0 dBz @ 20 km 1 m^2 @ 111 km	0 dBz @ 20 km 1 m^2 @ 111 km *	0 dBz @ 10 km 1 m^2 @ 370 km
Antenna				
Elevation Beamwidth	0.55 Degrees (min)	5 Degrees	5 Degrees	2 Degrees (stacked)
Azimuth Beamwidth	0.55 Degrees	1.4 Degrees	1.4 Degrees	1.4 Degrees
Power Gain	50 dB	34 dB	34 dB	35 dB (transmit), 40 dB (receive)
Rotation Rate	5 RPM (max)	12.5 RPM	12.5 RPM	5.0 RPM
* 17dB sensitivity reduction in short-pulse processing range (0 - 6.5 nmi)				

2.2.1 Airport Surveillance Radar 9

The ASR-9 radar system was introduced into operation by the FAA in 1990. This radar system is capable of multiple target detection [7]. It also has the capability to process weather information such as precipitation in six total levels ranging from light rain to severe thunderstorm [7]. The radar also has a secondary antenna attached to the primary detection antenna for transponder related communications with aircraft. This provides additional aircraft information and can act as a redundancy if the primary radar is not functioning properly [7]. The image in Figure 2.3 is the ASR-9 located at Tampa International Airport in Tampa, Florida.

Figure 2.3. Airport Surveillance Radar 9. Source: [8].

The figure shows the ASR-9 mounted on a pedestal, enabling maximum performance and clearance from ground level interference sources. The total ASR-9 radar count in operation exceeds 120 [7].

2.2.2 Airport Surveillance Radar 11

The ASR-11 radar system was implemented in 1998 as a replacement for the ASR-9 or to be installed at locations that did not receive the ASR-9 [9]. Additionally, the ASR-11 provided a much-needed update to airports still utilizing the 20-year-old legacy Air Surveillance

Radar 7 (ASR-7) and Air Surveillance Radar 8 (ASR-8) systems [9]. The digital processing and updated technology significantly increased performance, improved aircraft detection, and bolstered weather forecasting capability across the United States. Much like the ASR-9, the ASR-11 has both a primary and secondary radar system to detect and identify aircraft, respectively. It retains the six-level weather processing capability seen previously in the ASR-9 [10]. This radar is also mounted on a pedestal system and is shown in Figure 2.4.

Figure 2.4. Airport Surveillance Radar 11. Source: [9].

2.2.3 Terminal Doppler Weather Radar

Brought into service by the FAA in 1994, the TDWR was developed by the Massachusetts Institute of Technology (MIT) Lincoln Laboratory in response to airline crashes in the prior two decades due to excessive wind shear. Wind shear is caused by rapid changes in direction and speed of wind gusts, the most dangerous being downward wind shear [11]. The TDWR was incredibly successful at tracking and informing air traffic controllers of wind related conditions, so much so, that the FAA reports zero wind shear incidents at

airports employing the TDWR since 1994 [11]. The TDWR has been implemented at 46 high-throughput airports within the U.S. and Puerto Rico [11]. Although this radar is not traditionally used to track aircraft, its operating specifications provide meaningful insight on how it could potentially perform if repurposed for aircraft detection and tracking much like the study being proposed here. Figure 2.5 shows the TDWR.

Figure 2.5. Terminal Doppler Weather Radar. Source: [12].

2.2.4 Airport Route Surveillance Radar 4

The ARSR-4 procurement was a joint venture by the DOD and FAA to develop a perimeter monitoring / defense of U.S. airspace. The U.S. Air Force maintains oversight of the ARSR-4 radar systems for military use, as these radars are an integral part of the many early warning detection capabilities of the DOD as a whole [13]. The first radar was commissioned into service in 1996 [14]. The ARSR-4 was developed by Northrop Grumman with both Air Traffic Control and Air Force design constraints, providing a distinct advantage over the legacy Air Route Surveillance Radar 3 (ARSR-3) it sought to replace in the mid-1990s [15].

Figure 2.6 shows the ARSR-4.

Figure 2.6. Airport Route Surveillance Radar 4. Source: [14].

2.3 Selected Target Aircraft

The necessity for inclusion of multiple target aircraft in this study is that aircraft of varying size and velocity provide comprehensiveness to objectives of this research. This enables the reader to develop intuition about how each radar system performs and what can be the best use cases for each one. Utilizing [4] as a basis for target selection, three targets are chosen. The RCS value and target speed are provided in Table 2.2.

Table 2.2. Target aircraft selection options. Source: [4].

No.	Aircraft Type	RCS	Speed (km/hour)
1.	Bell 47G	3	168.532
2.	F-16 Fighting Falcon	5	1470
3.	Hawk200	8	1,000.08
4.	Su-30 Sukhoi	15	2,878.75
5.	Cobra AH-1S	18	227.796
6.	Cassa C-212	27	364.844
7.	CN-235	30	459.296
8.	A-310 Airbus	100	980

From Table 2.2, three aircraft were chosen: Lockheed Martin F-16 Fighting Falcon, Construcciones Aeronáuticas SA CN-235, and Airbus A310. These selections provide a variety of RCS values and target speeds as originally desired.

2.3.1 Lockheed Martin F-16 Fighting Falcon

The Lockheed Martin F-16 Fighting Falcon (F-16) is the fastest and lowest observable target aircraft utilized in this research. It is a staple aircraft in many allied militaries around the world, with over 2180 active aircraft amongst seven total countries. The U.S. currently employs 936 of the total number of active aircraft [16]. The F-16 has been in active service since 1979, with improvements and variants employed over the years. The F-16 is 9.8 m in wingspan, 14.8 m in length, and 4.8 m in height [17]. The full aircraft and three-view diagram are shown in Figure 2.7 and Figure 2.8, respectively.

Figure 2.7. Lockheed Martin F-16 Fighting Falcon. Source: [17].

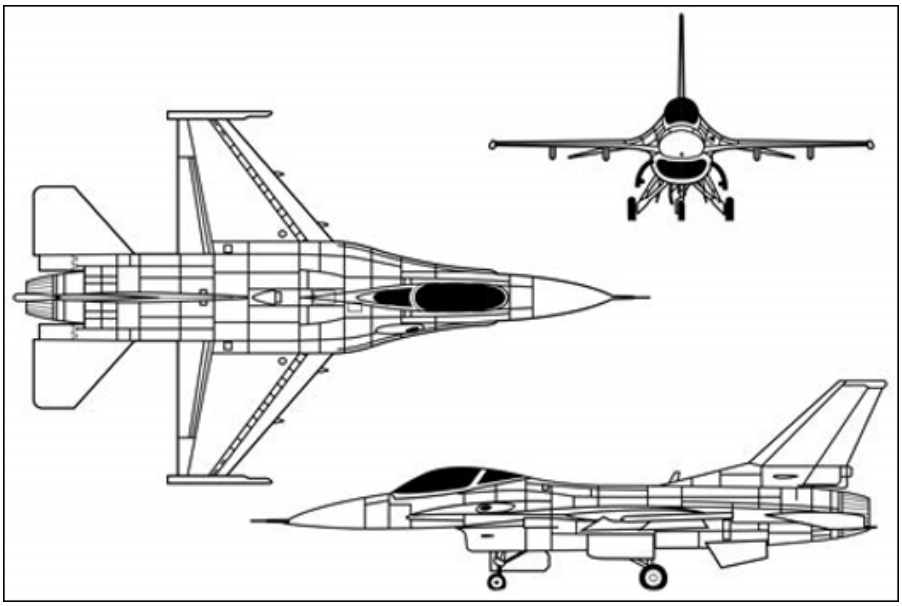

Figure 2.8. Lockheed Martin F-16 Fighting Falcon, three-view. Source: [18].

2.3.2 Construcciones Aeronáuticas SA CN-235

The Construcciones Aeronáuticas SA CN-235 (CN-235) stands as the mid-size aircraft in this research. It is the second largest, but slowest moving target aircraft of the three. This aircraft is a medium-lift military aircraft, with a maximum payload of 5950 kg [19]. The CN-235 was introduced into service in 1988, with 273 total produced, and has been flown by 29 countries including the U.S. [20]. This aircraft has a wingspan of 25.8 m, a length of 21.4 m, and a height of 8.17 m [19]. The full aircraft and three-view diagram are shown in Figure 2.9 and Figure 2.10, respectively.

Figure 2.9. Construcciones Aeronáuticas SA CN-235. Source: [20].

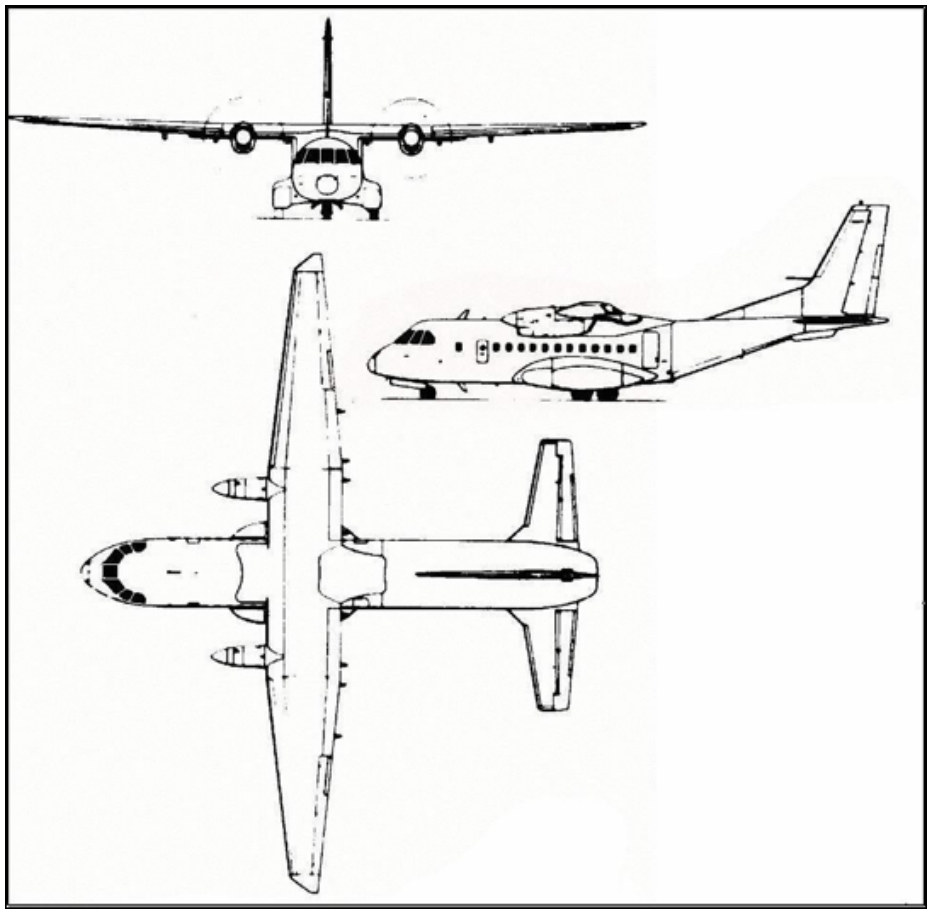

Figure 2.10. Construcciones Aeronáuticas SA CN-235, three-view. Source: [21].

2.3.3 Airbus A310

The final aircraft selected for this study is by far the largest, and out of the three chosen aircraft, is second fastest. The Airbus A310 (A310) has been in service since 1983 but has been largely phased out in the industry [22]. As an example, FedEx Express retired its final A310 in January 2020 out of a fleet total 70 aircraft [23]. The A310 is a popular aircraft amongst commercial passenger carriers and air freight companies alike. Typical passenger count varies between 190 and 230 depending on seating layout [22]. The A310 is 43.9 m in wingspan, 46.6 m in length, and 15.8 m in height [22]. The full aircraft and three-view

diagram are shown in Figure 2.11 and Figure 2.12, respectively.

Figure 2.11. Airbus A310. Source: [24].

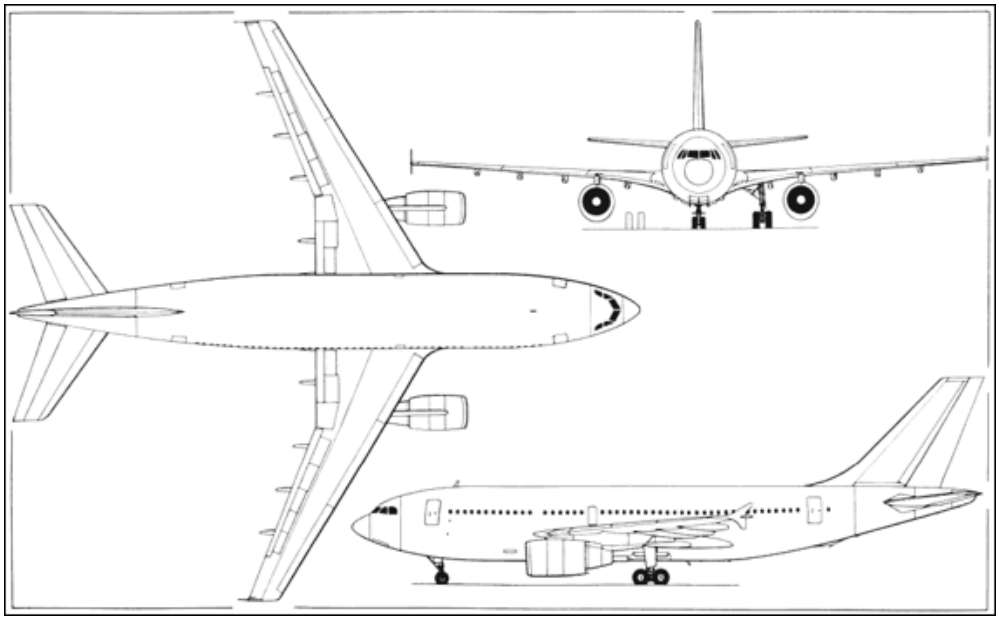

Figure 2.12. Airbus A310, three-view. Source: [25].

CHAPTER 3:
Performance Comparison and Analysis Setup

3.1 Assumptions and Constraints

To facilitate the performance comparison between radar systems, parameter specifications are needed as inputs to the Matlab simulation program including some of the parameters from Table 2.1. Additionally, target RCS and velocity specifications are used from Table 2.2 for each aircraft.

To reduce complexity and provide consistency to the comparison, some assumptions and constraints are applied. Regarding the target aircraft, two constraints are applied. First, the RCS of each aircraft is strictly an estimate based on [4] and is assumed to be oriented with the nose of the aircraft facing directly towards the radar. This constraint also assumes line-of-sight to the target at all detection ranges and ignores multi-path and atmospheric refraction. Second, and related to the first point, the aircraft flies along a fixed angle of approach towards the radar in order to capture that RCS. This also has implications for Doppler frequency calculations, as the orientation of the aircraft flight path relative to the radar on the ground is considered. In calculating for the maximum Doppler frequency, an aircraft is assumed to fly directly into the airport, (i.e., the target enters the main lobe of the radar antenna) or directly away from it, which is clearly radial direction. Any angular deviation from this radial direction will net a lower Doppler frequency.

In the radar range equation (RRE) to be discussed in the next section, the loss term, L, refers to the total system losses. In the conventional use of the FAA radars, the weather-related factors such as water droplets are actually targets of interest and are not considered losses. In our objectives that solely consider aircraft targets, rain drops and the like constitute SNR loss due to propagation effects on the radar waves. For a fair comparison between radars, a maximum total of 10 dB system loss is applied to all radar systems. There is one exception: a low-loss case, 3 dB, is investigated with the F-16 to compare the results of the initial 10 dB loss case against a reduced loss term (that may constitute a clear day). The 10 dB system loss number will be otherwise consistent for the remainder of the comparison study. The

noise figure values utilized for each radar are as follows: ASR-9 is 4 dB [26], ASR-11 is 2.3 dB [27], TDWR is 1.4 dB [28], and ARSR-4 is 3.6 dB [26]. Regarding range considerations, it assumed that aircraft is in the main lobe of the radar antenna. Clearly, if the aircraft is not directly in the center of the main, detection range is reduced and will be discussed further. For Doppler frequency calculations, the maximum velocity of the aircraft is used. Lastly, the comparison requires a radar system detection SNR threshold, of which the value of 13 dB (approximately 20 in decimal) is selected. Older radars typically employ non-coherent receivers and it is likely that these FAA radars employ the same technique which also means a high SNR required, where typically 16 dB or above is used. Recall that our goal is to extend these radars to employ modern coherent receiver processing. The advantage of switching from non-coherent method to coherent technique is either increase in system performance or a decrease in transmit power required since the SNR requirement is lowered. The typical starting SNR estimate for coherent receiver processing is 13 dB.

3.2 SNR vs. Range Calculation

The first set of comparison results is the SNR vs. target range performance curves for the various radars. Using all previously introduced radar specifications, assumptions, and constraints, a SNR vs. range curve for each radar is reported. The SNR is given by the traditional RRE which is shown in (3.1).

$$SNR = \frac{P_r}{P_n} = \frac{P_t G_t G_r \lambda^2 \sigma_{RCS}}{(4\pi)^3 R^4 F k_o L T_o B} \tag{3.1}$$

The variables P_t, P_r, and P_n represent transmitted, received, and noise power, respectively. G_t and G_r are the transmit antenna gain and receive gain. λ is the wavelength of the transmitted carrier signal and σ_{RCS} is the RCS of the aircraft or target. In the denominator, F is the noise figure, k_o is the Boltzmann constant, L represents the total system loss, T_o is the standard noise temperature, and B is the bandwidth of the transmitted signal. When all the performance curves are plotted together and a desired SNR detection threshold (SNR_{req}) is utilized, the maximum detection range (R_{max}) is easily found for each radar. The SNR vs. range curves for each aircraft will be reported later in Chapter 4.

3.3 Range vs. RCS Calculation

In this portion of the study, aircraft range from the radar is calculated as RCS is varied from (almost) zero to 100 m^2. In other words, the maximum detection range as a function of RCS is dictated by (3.2) by re-arranging (3.1).

$$R_{max} = \sqrt[4]{\frac{P_t G_t G_r \lambda^2 \sigma_{RCS}}{(4\pi)^3 (SNR_{req}) F k_o L T_o B}} \tag{3.2}$$

As indicated before, detection range is designated maximum in the sense that it corresponds to the detection SNR threshold and assumes the peak antenna main beam gain. Detection range corresponding to HPBW gain will be determined and annotated in a later section.

3.4 Doppler Frequency Calculation

Doppler frequency is necessary to understand the effects of target velocity on radar performance. The equation for Doppler frequency is shown in (3.3).

$$F_D = \left| \frac{2v \cos \psi}{\lambda} \right| \tag{3.3}$$

The variable v represents target velocity, ψ represents angular deviation between target flight path and transmitted radar pulse, and λ is the wavelength of the transmitted pulse as in (3.1). In other words, if a target traveling radially towards the radar then the angular deviation is zero, and thus in (3.3), the maximum velocity corresponds to maximum Doppler frequency [5]. Additionally, a target traveling perpendicular to the radar system returns zero Doppler, as the direction of travel has no component in the radar pulse direction of travel. A visual representation of the Doppler frequency calculation is shown in Figure 3.1.

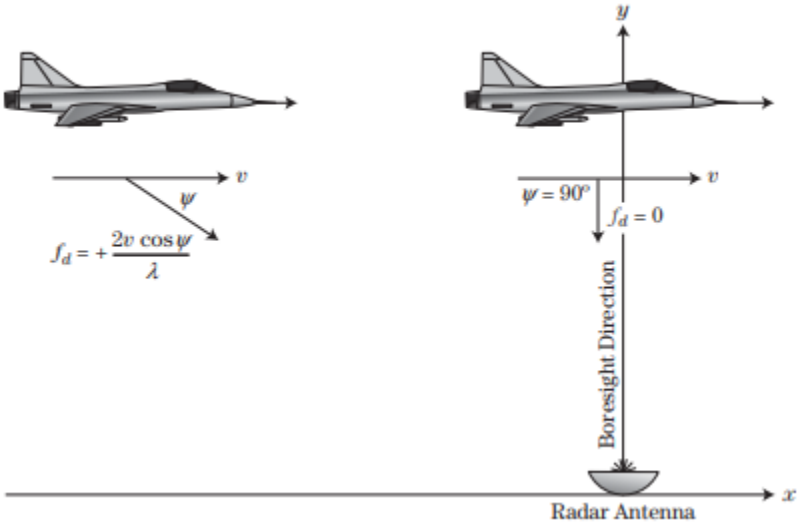

Figure 3.1. Doppler frequency example, showing two instances of aircraft Doppler frequency calculations. Source: [5].

According to the Nyquist sampling theorem, a sampling frequency of a receiver must be greater than or equal to twice the maximum frequency of the signal intended to be sampled to prevent aliasing. In radar systems, if the Doppler frequency received from a target is greater than half the pulse repetition frequency (PRF), then target velocity aliasing will occur. Given a target traveling at a velocity large enough to result in Doppler aliasing, the radar system may have a difficult time determining the target aircraft velocity as it processes the incoming signal. In the next chapter, the resulting Doppler frequency of each radar system is plotted against the target aircraft velocity, with the accompanying velocity threshold set to match the aircraft maximum velocity. This provides the reader with a visual comparison of not only the specific target Doppler frequency, but also illustrate how each radar's received Doppler frequency is affected by an interval of possible velocity values.

3.5 Radar Beam Comparison Calculations

As a visual aid, radar beams are plotted according to their relative beamwidths together with the maximum target detection range for all the radars under consideration. Each beam is

tilted upwards in elevation to show the entire beam above the horizon. Both the maximum detection range and the HPBW detection range are delineated in the figure legend for straightforward comparison. To form each beam, some preliminary calculations must be made. First, the minimum detectable signal must be determined with (3.4).

$$S_{min} = (SNR_{req})Fk_oT_oB \tag{3.4}$$

Next, the detection ranges must be calculated. In order to correctly form the beam, the center beam value and HPBW detection range value must be determined. The HPBW is defined as the beam edge for this comparison. As one may expect, a beam plot with only three points (HPBW, center beam, HPBW) would not adequately capture each radar beam curvature. This would reduce the quality of comparison. As a result, an intermediate value is added on each side of the center beam value, so the resulting beam is formed as follows: HPBW, intermediate point, center beam, intermediate point, and HPBW. This pattern sufficiently depicts each unique beam with enough detail to make a visual comparison and (3.5) represents the calculation necessary for each point on the radar beam.

$$R_{max} = \sqrt[4]{\frac{P_t(\alpha G_t)(\alpha G_r)\lambda^2\sigma_{RCS}}{(4\pi)^3(SNR_{req})Fk_oLT_oB}} \tag{3.5}$$

Equation 3.5 is used, with the variable α varied for each case; 0 dB for the antenna center beam, -1.5 dB for an intermediate point on the antenna beam, and -3 dB for HPBW. All variables remain the same as described in (3.2). The α term is seen twice in (3.5) in order to correctly capture the effect of a two-way loss, as radars must account for a loss in the transmit gain and receive gain for a target detected outside the center beam of the antenna.

Now that the respective detection ranges are determined, they are marked to the corresponding place on the beam when presented in the next chapter. These beams are then plotted in such a way to show an elevation view of the beams with pertinent range information contained in the legend. The beams are tilted upward in elevation such that the entire beam is above the horizon. Of note, only the center beam and HPBW values are specified in the figure, as an intermediate value is not commonly used when describing antenna beams formed by radar systems.

3.6 Time to Arrival Calculation

Another useful metric to compare radar system detection performance is to determine the time to arrival (TTA) of the target aircraft to the location of the radar. Since these radars are generally located within proximity, if not in the center of airport / airfield grounds, TTA is the amount of time remaining before a target aircraft arrives for landing. TTA clearly depends on how far the aircraft is from the airport and the approaching velocity. Here, we are interested in the TTA corresponding to the detection range (center beam or HPBW) in kilometers, and the target aircraft velocity in km/s. Given the anticipated detection range, the time in minutes is dictated by (3.6). If the unit second is desired, the factor of 60 in the denominator is omitted.

$$TTA = \frac{R_{max}}{60v} \tag{3.6}$$

Intuitively, this time will provide the fastest possible TTA since maximum aircraft velocity is used. Of course, in reality, aircraft generally do not fly at maximum velocity at all. However, this provides a consistent basis for comparison and remains in concurrence with the assumption that the aircraft travels along a fixed flight path and velocity as it approaches the radar system. If the radar were to miss the target and eventually detect it after one complete rotation, then the TTA value would decrease linearly as a function of the rotation rate since the target travels at a fixed velocity.

3.7 Maximum Possible Number of Radar Pulses

In addition to the single transmitted pulse comparison, a study that provides greater performance with the use of the multiple pulses is investigated as per our motivation. In order to develop a performance comparison, the maximum possible number of pulses in an antenna beamwidth is calculated for each radar system.

The beam rotation rate, typically specified in revolutions per minute, is denoted by ω. This beam rotation rate needs to be converted into a scan rate, $\frac{d\theta_s}{dt}$, in the units of degrees per second. The conversion is shown in (3.7).

$$\frac{d\theta_s}{dt} = 6\omega \tag{3.7}$$

Equation 3.8 provides the amount of time, in seconds, that the radar spends within each

azimuth beamwidth, θ_B, as it rotates.

$$t_{ot} = \frac{\theta_B}{\frac{d\theta_s}{dt}} = \frac{\theta_B}{6\omega} \tag{3.8}$$

The calculation to determine maximum possible number of pulses is given by (3.9).

$$N_P = t_{ot} PRF = \frac{\theta_B}{6\omega} PRF \tag{3.9}$$

The variable PRF is termed as the pulse repetition frequency. As a reminder, the resulting value in (3.9) is rounded down to the nearest whole number such that complete pulses are integrated in the receiver.

With the use of N_P, for each radar, the SNR vs. range, range vs. RCS, and beam comparison figures are generated. The only exception is the Doppler frequency since Doppler shift is not directly affected by maximum number of pulses received. To account for the number of pulses in the SNR version of the RRE equations, N_P is multiplied to the transmit power wherever it is used in order to capture the full integrated power. In this work, recall that the motivation is to increase detection performance of the radars, as such the maximum number of pulses is used instead of a much less effective number of pulses typically used in legacy radars. Prior to inspecting the performance results in the next chapter, it is noted that the total number of performance figures per target aircraft is seven.

THIS PAGE INTENTIONALLY LEFT BLANK

CHAPTER 4:
Analysis and Results

This chapter reports the performance curves, beam comparisons, and other analysis results for the F-16, CN-235, and A310 aircraft. For consistency, the line colors (in the resulting performance figures throughout this chapter) associated with a particular radar system will remain the same. The ASR-9 performance curves are shown in orange, the ASR-11 curves are shown in teal for short pulse and blue for long pulse, the TDWR curves are shown in maroon, and the ARSR-4 curves are shown in green. To organize the results of the analysis, each section containing performance curves corresponding to a particular aircraft includes seven total figures and is followed by one table in order to consolidate and summarize results. Like the figures, all tables are formatted identically to aid in expeditious comparison. In this chapter, range is described in units of kilometers. The term *single pulse* refers to results using one pulse transmission while *maximum number of pulses* will refer to results with the use of the maximum possible number pulses within a single beamwidth.

4.1 F-16 Simulation Results

4.1.1 SNR vs. Range – Single Pulse

The single pulse transmission comparison is important in order to gain intuition about how the radar specifications impact detection capability without the use of multiple pulses with its corresponding integration gain. The number of pulses may vary depending on a given radar and thus a single pulse comparison acts a starting baseline. The first aircraft to be analyzed is a low observable aircraft with a single digit RCS. Although the F-16 was described in great detail in Chapter 2, the parameters needed for this comparison study are the aircraft RCS and maximum velocity. These values are 5 m^2 and 408.3 m/s, respectively. Figure 4.1 shows SNR vs range for a single pulse transmission with received SNR in dB and the range in kilometers. A dashed line is included to delineate the selected detection SNR threshold that corresponds to the maximum detection range for both the upper and lower plots.

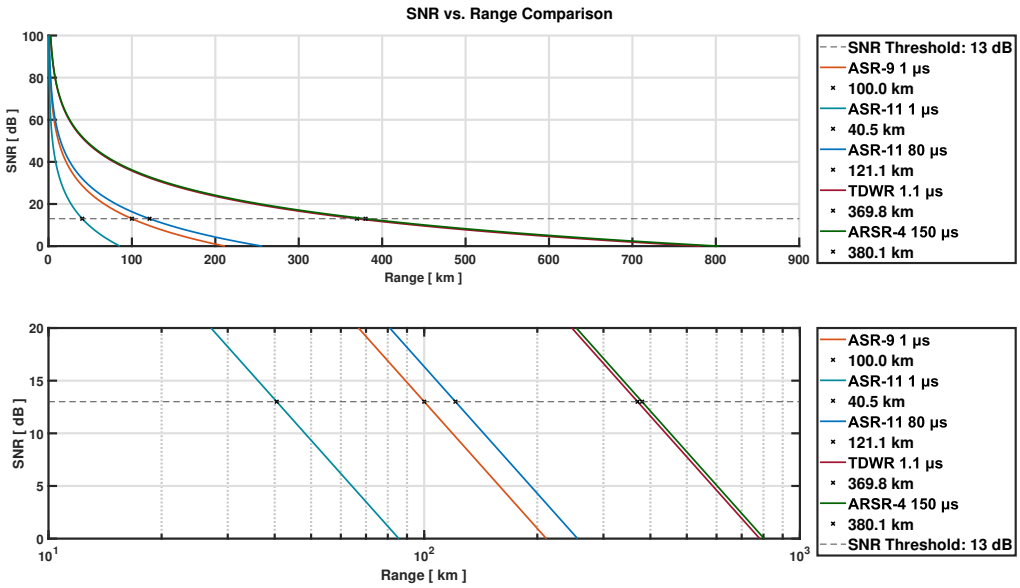

Figure 4.1. SNR vs. range with single pulse transmission for F-16.

In Figure 4.1, note that the x-axis (range) of the lower plot is shown in logarithmic scale, which aids to visually separate the performance curves for easy comparison. The resulting SNR vs. range performance curves are illustrated as dictated by (3.1), which shows that SNR decreases as the target range increases. The ASR-11 short pulse, shown in teal, has the lowest maximum detection range at only 40.5 km range. The next two performance curves, orange and blue, are close together where the maximum detection ranges are at 100 km and 121.1 km, respectively. Recall that the ASR-9 power level is 1.1 MW with a 1 µs pulse width and the ASR-11 power level is 20 kW with a much longer pulse of 80 µs. Despite the differences in pulse and power, it is interesting to note that these two systems have similar performance in detecting the F-16. The next two radars have nearly identical performance, as their curves are nearly on top of each other. The TDWR has a maximum detection range at 369.8 km while the ARSR-4 has a maximum detection range of 380.1 km.

4.1.2 SNR vs. Range – Maximum Number of Pulses

This section remains focused on SNR vs. range and considers the maximum number of radar pulses determined in (3.9). The resulting SNR vs. range performance curves are shown in Figure 4.2.

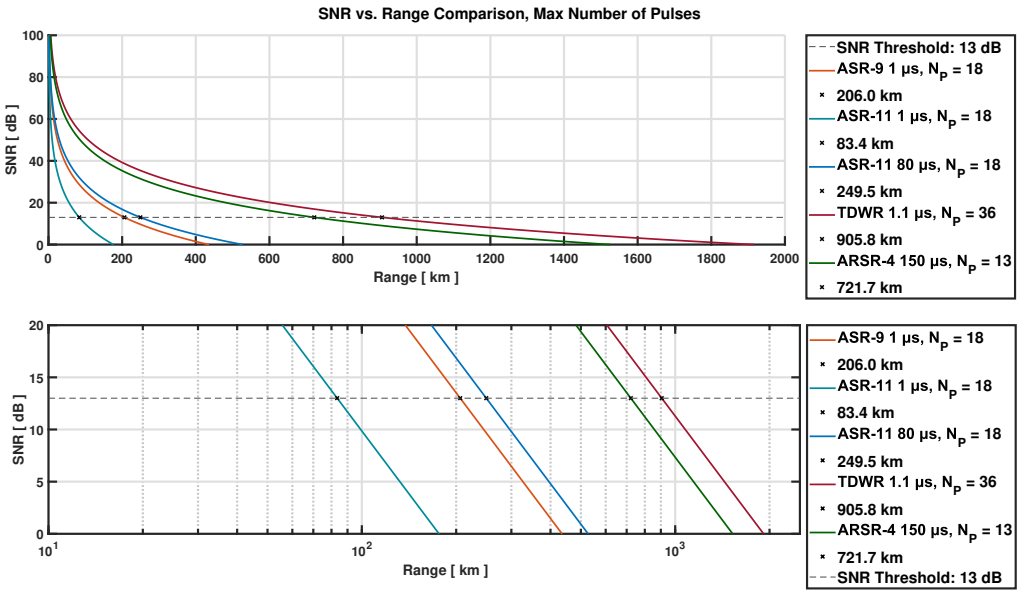

Figure 4.2. SNR vs. range with transmission of maximum number of pulses for F-16.

In Figure 4.2, the performance curves follow expected SNR vs. range relationship. Of note, the number of pulses, denoted in the figure legend as N_P, approximately doubles the detection range. For example, the ARSR-4 single pulse detection range is 380.1 km while $N_p = 13$ results in a detection range of 721.8 km. The most interesting result of transmission of maximum number of pulses is that the TDWR has the best SNR vs. range performance curve. Previously in the single pulse transmission case, the ARSR-4 provided a larger detection range as compared to the single pulse results.

4.1.3 Beam Comparison – Single Pulse

Following the process outlined in Chapter 3 for forming the radar beams and utilizing the detection ranges from the SNR performance curves for the center beam antenna gain, the single pulse transmission beam comparison is shown in Figure 4.3.

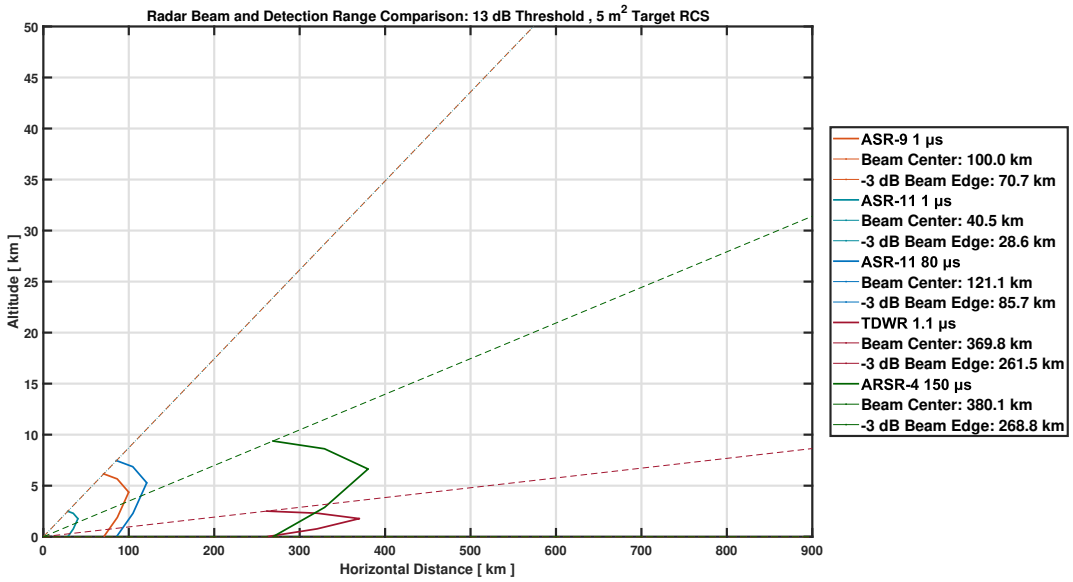

Figure 4.3. Radar beam comparison with single pulse transmission for F-16.

Figure 4.3 shows the elevation angle of the beams, with respect to the other side of the beam, which is placed on the horizontal axis while the upper side of each beam is illustrated with the color-coded dashed line. The placement of each beam in the figure corresponds to the detection performance for each specified aircraft. Breaking the elevation beamwidth into four parts, the HPBW detection ranges are placed on the upper and lower beam edges and the center beam detection range is placed in the center of the beam, while the intermediate ranges are in between. A radar antenna tilt, unique to each radar, is applied in order to raise the entire beam above the x-axis or horizon as part of our motivation to extend capabilities of these radars. The ASR-9 and ASR-11 both share the same elevation beamwidth of five degrees, explaining why the beams are similar in shape and there seems to be only three dashed lines, even though four radar systems are compared. One important note is that

the HPBW detection ranges are included in the legend labels for each radar. From left to right, the order of the beams match what was determined by the previous SNR vs. range calculations: ASR-11 short pulse, ASR-9, ASR-11 long pulse, TDWR, and the ARSR-4 being the top performer. The TDWR and ARSR-4 have almost identical detection ranges with respect to the single pulse transmission. For reference, the elevation beamwidths of the TDWR and ARSR-4 are 0.55° and 2°, respectively. TTA values are calculated from the center beam detection range in the single pulse transmission and are reported as: 1.7 min for ASR-11 short pulse, 4.1 min for ASR-9, 4.9 min for ASR-11 long pulse, 15.1 min for TDWR, and 15.5 min for ARSR-4.

4.1.4 Beam Comparison – Maximum Number of Pulses

Based on the SNR vs. range calculations, it is anticipated that the detection ranges for the TDWR will outperform the ARSR-4. This prediction is confirmed in Figure 4.4.

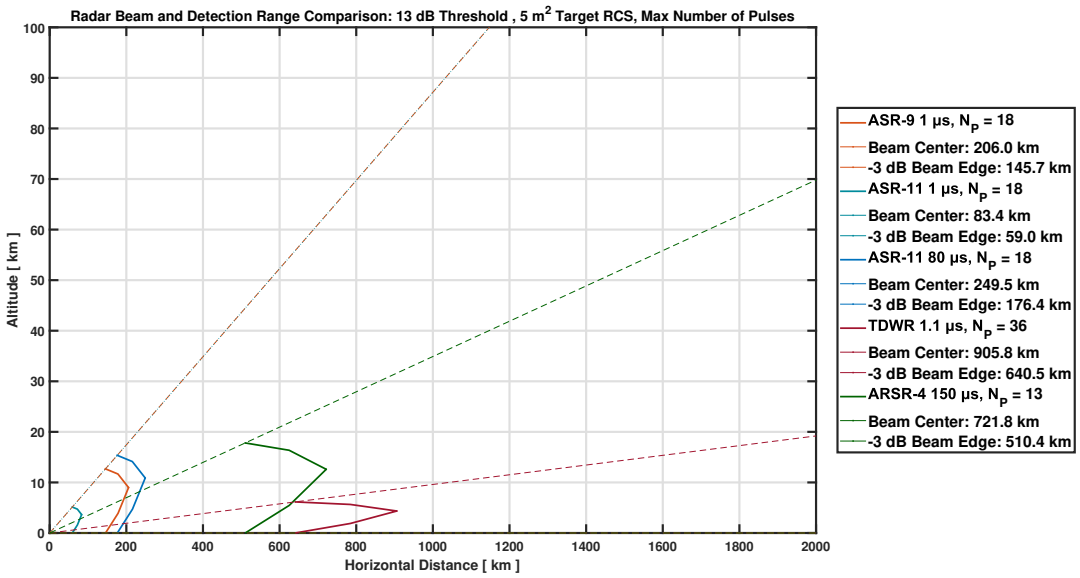

Figure 4.4. Radar beam comparison with transmission of maximum number of pulses for F-16.

From left to right, the order of the radar beam performance is: ASR-11 short pulse, ASR-9,

ASR-11 long pulse, ARSR-4, and the TDWR. Additionally, the detection ranges match the expected ranges corresponding to the maximum number of pulses from Figure 4.2. TTA corresponding to the detection range with the maximum number of pulses via center beam are: 3.4 min for ASR-11 short pulse, 8.4 min for ASR-9, 10.2 min for ASR-11 long pulse, 29.5 min for ARSR-4, and 37 min for TDWR.

4.1.5 Range vs. RCS – Single Pulse

Another metric for radar comparison is detection range as a function of the RCS of the target. Given a required SNR, the performance curve is shown in range vs. RCS. Thus, given some aircraft RCS, the corresponding detection range can easily be found. This is especially important for the DOD, as the ability to quickly correlate target RCS to detection range enables rapid decision-making about how to best neutralize a potential threat. The resulting range vs. RCS performance curve also considers a scenario where the current target's RCS is reduced due to the orientation of the target relative to the radar beam. Figure 4.5 depicts the performance curves corresponding to the single pulse transmission where the lower figure's x-axis is in logarithmic form.

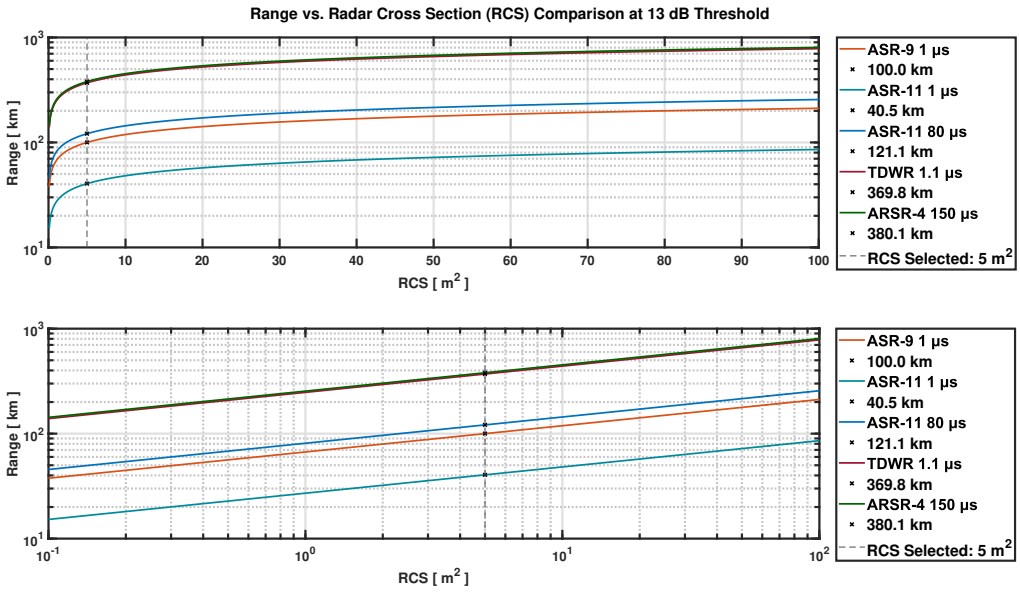

Figure 4.5. Range vs. RCS comparison with single pulse transmission for F-16.

The resulting order of radar performance is consistent with previous SNR vs. range and beam comparison figures. The ARSR-4 provides the highest detection range, and the ASR-11 short pulse provides the lowest. The utility of the logarithmic scale is appreciated most when the target has a RCS less than two square meters.

4.1.6 Range vs. RCS – Maximum Number of Pulses

The range vs. RCS performance curve shape corresponding to maximum number of pulses follows the curves in Figure 4.5. The detection range corresponding to the maximum number of pulses matches the expected increase in detection range unique to each radar as illustrated in Figure 4.6.

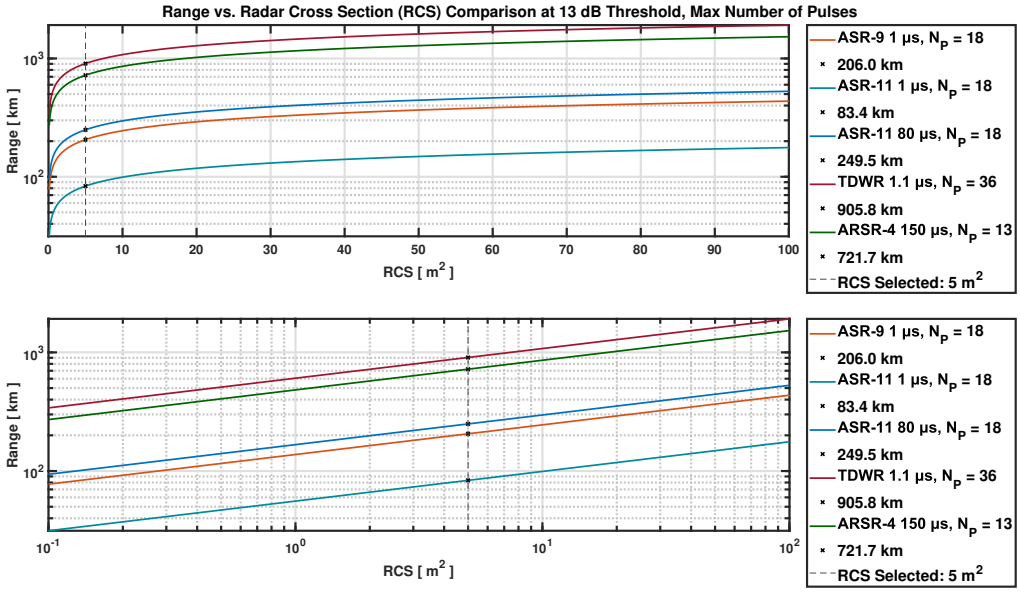

Figure 4.6. Range vs. RCS comparison with transmission of maximum number of pulses for F-16.

The performance curves corresponding to maximum number of pulses in Figure 4.6 follows the order of performance in Figure 4.2. The TDWR now provides the best performance instead of the ARSR-4, while the detection range of the ASR-11 short pulse duration remains the lowest.

4.1.7 Doppler Frequency Comparison

The final metric for comparison of radar systems in this research focuses on the target aircraft velocity which results in Doppler frequency shift assuming the aircraft is traveling in the radial direction towards the radar. The target aircraft maximum velocity is used to calculate maximum Doppler which is also a function of the operating frequency of the radar as dictated by (3.3). Figure 4.7 presents the Doppler frequency vs. target velocity curves for the four radar systems.

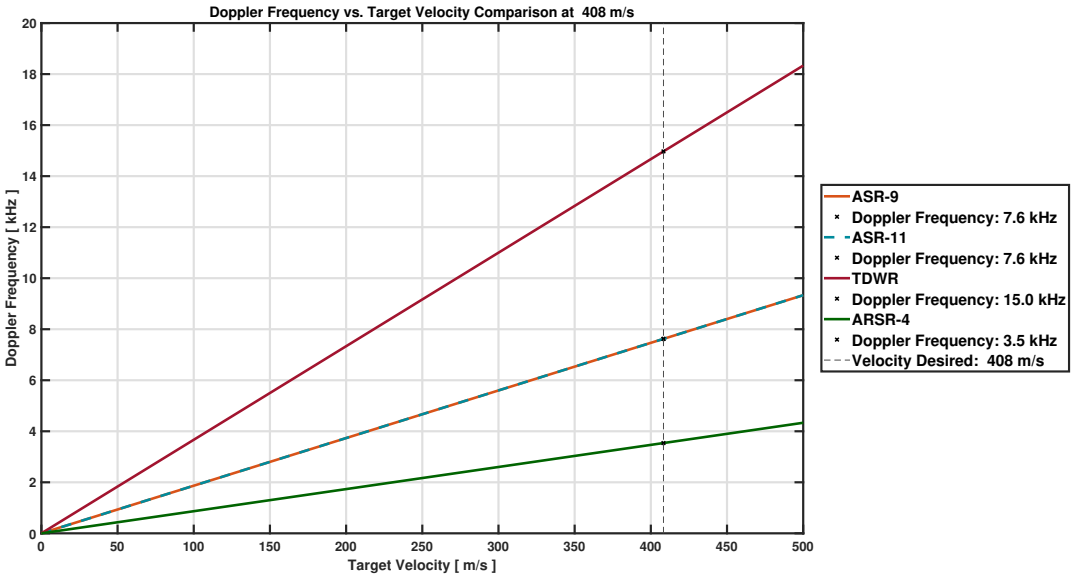

Figure 4.7. Doppler frequency vs. target velocity for F-16.

Note that the ASR-9 and ASR-11 have the same Doppler vs. target velocity profile. This is because the radar systems share the same operating frequency, thus (3.3) yields the same curve. Since TDWR carrier frequency is the largest (5.5 GHz), the Doppler vs. target velocity profile slopes the highest. The ARSR-4 operates at 1.3 GHz which is the lowest of all the carrier frequencies and thus offer the lowest observable Doppler.

4.1.8 F-16 Low-Loss Performance Results

This portion of the study investigates the effects on detection range and TTA where the loss term in (3.1) is reduced from 10 dB to 3 dB. All parameters other than L in the RRE remain the same for this comparison. For example, this low loss case may pertain to a clear day scenario.

SNR vs. Range - Single Pulse, Low-Loss

The reduction in loss by 7 dB results in an increased range at the 13 dB detection threshold. Resulting performance curves are similar to Figure 4.1. The range improvements compared

to the 10 dB loss case are as follows: 20.1 km for ASR-11 short pulse, 49.6 km for ASR-9, 60 km for ASR-11 long pulse, 183.2 km for TDWR, and 188.3 km for ARSR-4. Figure 4.8 reports the SNR vs. range results.

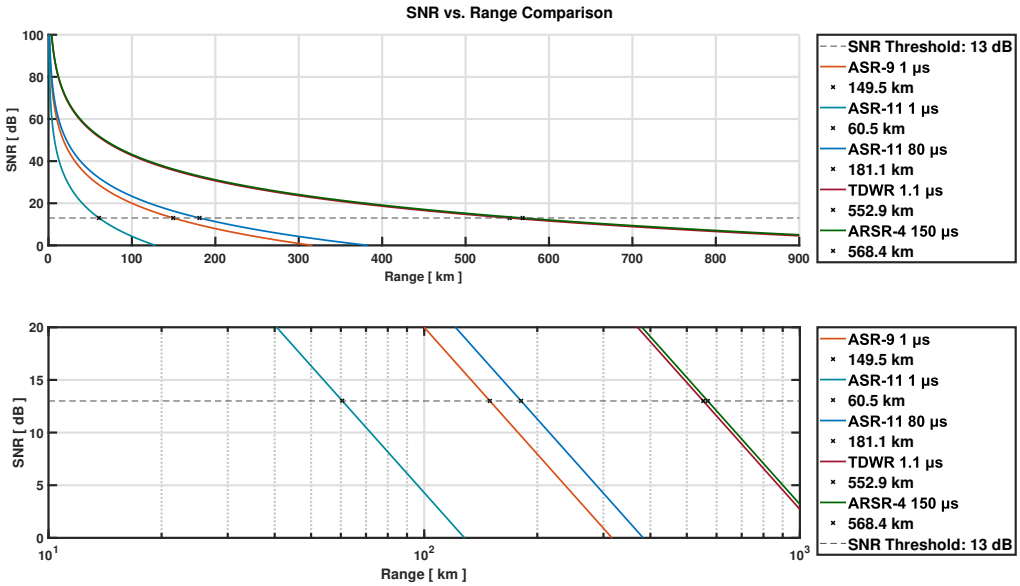

Figure 4.8. SNR vs. range with single pulse transmission for F-16, 3 dB loss.

SNR vs. Range - Maximum Number of Pulses, Low-Loss

The low loss of 3 dB also improves the detection range corresponding to the maximum number of pulses as compared to the 10 dB loss case in Figure 4.2. The range improvements due to reduced loss are as follows: 41.4 km for ASR-11 short pulse, 102.1 km for ASR-9, 123.6 km for ASR-11 long pulse, 357.5 km for ARSR-4, and 448.8 km for TDWR. Resulting performance curves are shown in Figure 4.9.

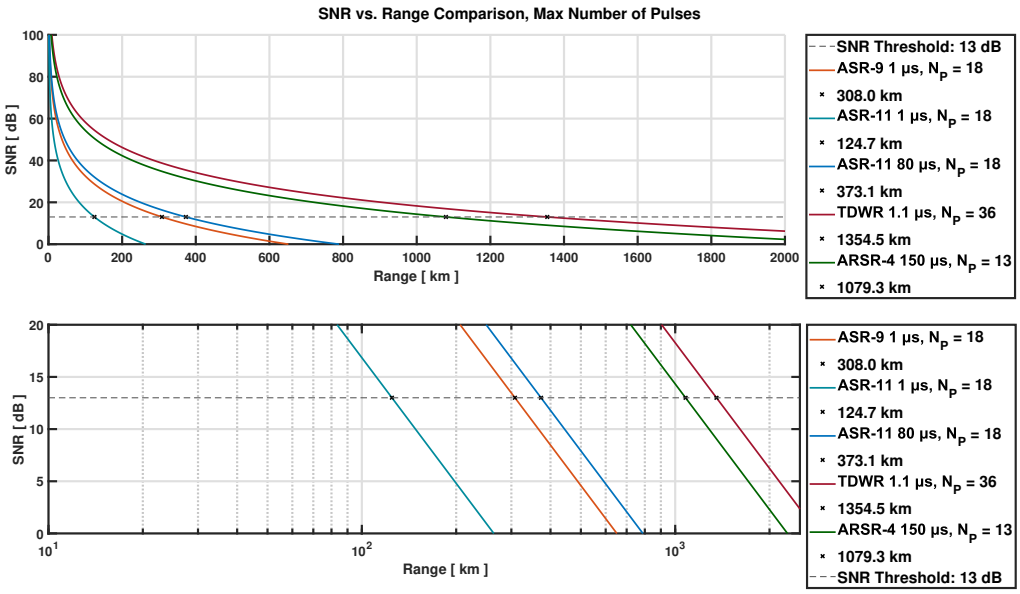

Figure 4.9. SNR vs. range with transmission of maximum number of pulses for F-16, 3 dB loss.

Beam Comparison – Single Pulse, Low-Loss

With the single pulse transmission utilizing 3 dB loss, the order of radar beams from left to right is the same as Figure 4.3. The increased detection range is shown in Figure 4.10. TTA improvements over the 10 dB loss case are as follows: 0.8 min for ASR-11 short pulse, 2 min for ASR-9, 2.5 min for ASR-11 long pulse, 7.5 min for TDWR, and 7.7 min for ARSR-4.

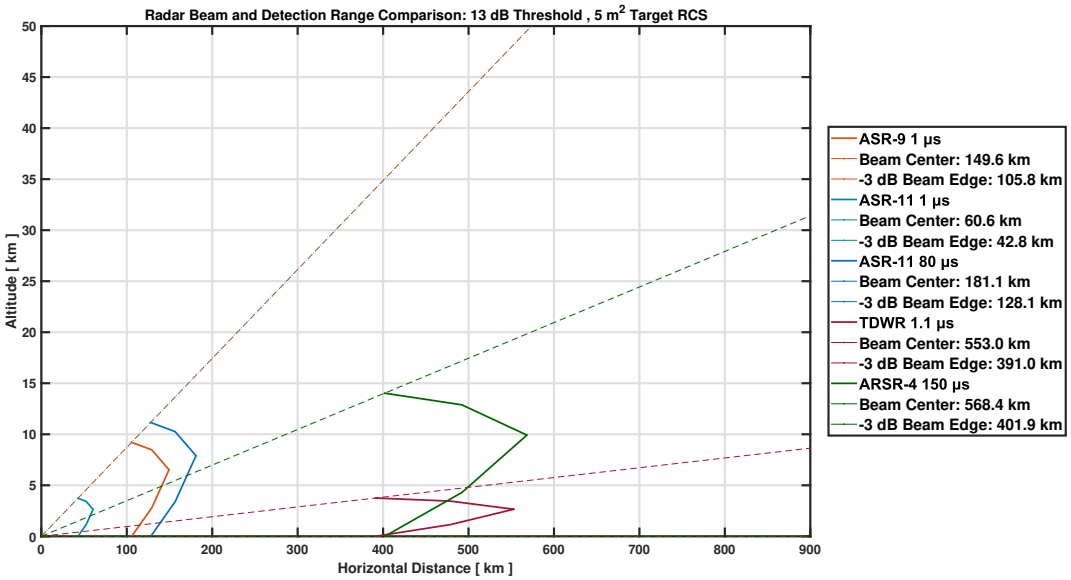

Figure 4.10. Radar beam comparison with single pulse transmission for F-16, 3 dB loss.

Beam Comparison – Maximum Number of Pulses, Low-Loss

For the maximum number of pulses comparison utilizing 3 dB loss, the order of radar beams from left to right is the same as Figure 4.4. The increased detection range is shown in Figure 4.11. TTA improvements over the 10 dB loss case are as follows: 1.7 min for ASR-11 short pulse, 4.2 min for ASR-9, 5 min for ASR-11 long pulse, 14.6 min for ARSR-4, and 18.3 min for TDWR.

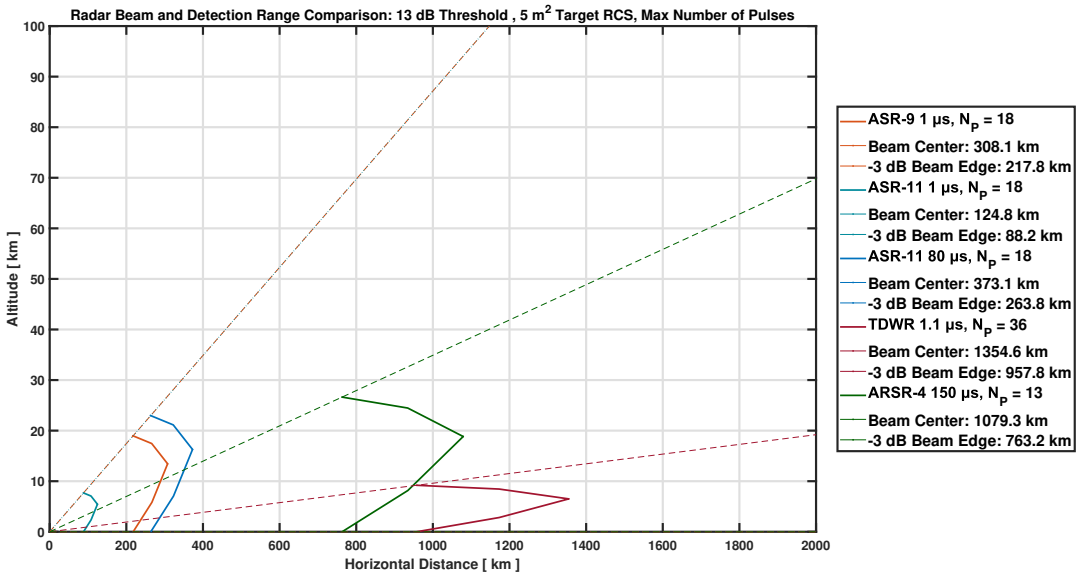

Figure 4.11. Radar beam comparison with transmission of maximum number of pulses for F-16, 3 dB loss.

Range vs. RCS – Single Pulse, Low-Loss

The detection range vs. RCS performance curves are improved by the decrease in loss from 10 dB to 3 dB as expected. Single pulse comparison is shown in Figure 4.12.

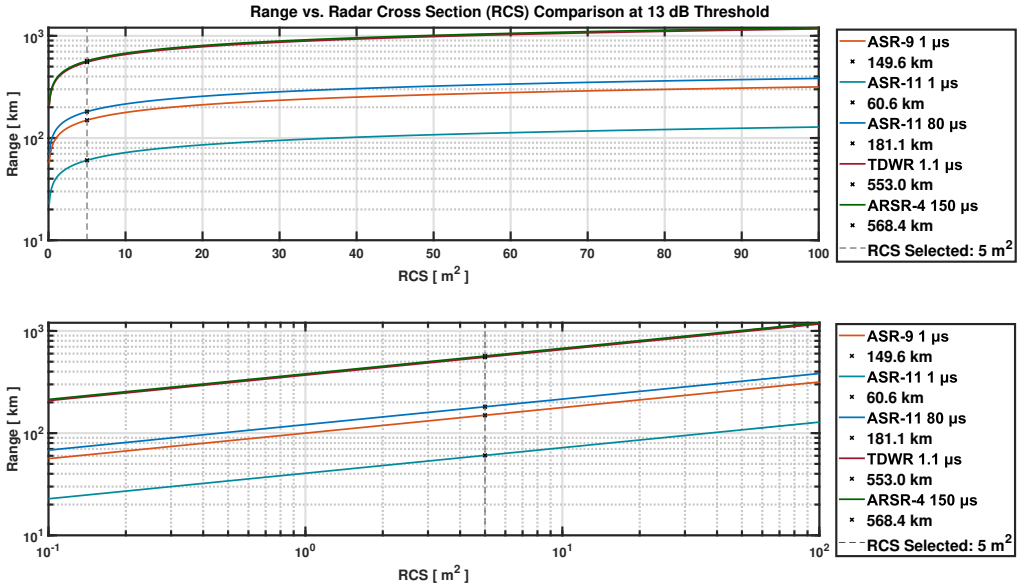

Figure 4.12. Range vs. RCS comparison with single pulse transmission for F-16, 3 dB loss.

Range vs. RCS – Maximum Number of Pulses, Low-Loss

The detection range vs. RCS performance curves are improved by the decrease in loss from 10 dB to 3 dB as expected. Additional range improvements result from the maximum number of pulses and are shown in Figure 4.13.

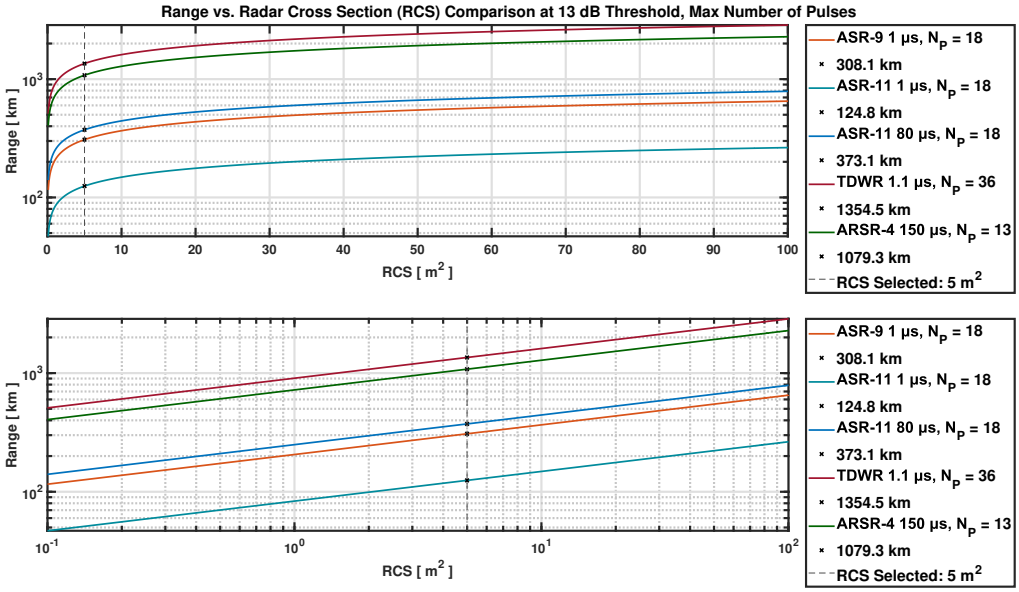

Figure 4.13. Range vs. RCS comparison with transmission of maximum number of pulses for F-16, 3 dB loss.

4.2 F-16 Summary

In this section, radar performance curves are reported corresponding to the F-16. The detection ranges and TTA values provide time for multiple radar rotations for target detections as the aircraft approaches. A collection of the output parameters presented in this section is shown in Table 4.1. This table also includes the HPBW detection ranges and accompanying TTA values.

Table 4.1. F-16 summary of results.

F-16	Units	ASR-9		ASR-11				TDWR		ARSR-4	
Pulse Width	us	1.0		1.0		80.0		1.1		150.0	
N_{Pulses}	-	Single	18	Single	18	Single	18	Single	36	Single	13
R_{max}	**km**	**100.0**	**206.0**	**40.5**	**83.4**	**121.1**	**249.5**	**369.8**	**905.8**	**380.1**	**721.8**
TTA_{max}	min	4.1	8.4	1.7	3.4	4.9	10.2	15.1	37.0	15.5	29.5
R_{-3dB}	**km**	**70.7**	**145.7**	**28.6**	**59.0**	**85.7**	**176.4**	**261.5**	**640.5**	**268.8**	**510.4**
TTA_{-3dB}	min	2.9	5.9	1.2	2.4	3.5	7.2	10.7	26.1	11.0	20.8
R_{max} (Low-Loss)	**km**	**149.6**	**308.1**	**60.6**	**124.8**	**181.1**	**373.1**	**553.0**	**1354.6**	**568.4**	**1079.3**
TTA_{max} (LL)	min	6.1	12.6	2.5	5.1	7.4	15.2	22.6	55.3	23.2	44.1
R_{-3dB} (LL)	**km**	**105.8**	**217.8**	**42.8**	**88.2**	**128.1**	**263.8**	**391.0**	**957.8**	**401.9**	**763.2**
TTA_{-3dB} (LL)	min	4.3	8.9	1.7	3.6	5.2	10.8	16.0	39.1	16.4	31.2
$F_{doppler}$	kHz	7.6		7.6				15.0		3.5	
PRF	kHz	1.0		1.0				2.0		0.288	
Aliasing?	Y/N	Y		Y				Y		Y	

4.3 CN-235 Simulation Results

4.3.1 SNR vs. Range – Single Pulse

The second aircraft detection comparison uses a medium-sized aircraft with a moderate RCS. The CN-235 resembles a U.S. C-130 aircraft, a common personnel and equipment transporter across the DOD. The RCS and aircraft velocity values are 30 m^2 and 127.7 m/s, respectively. Figure 4.14 shows SNR vs. range performance curves.

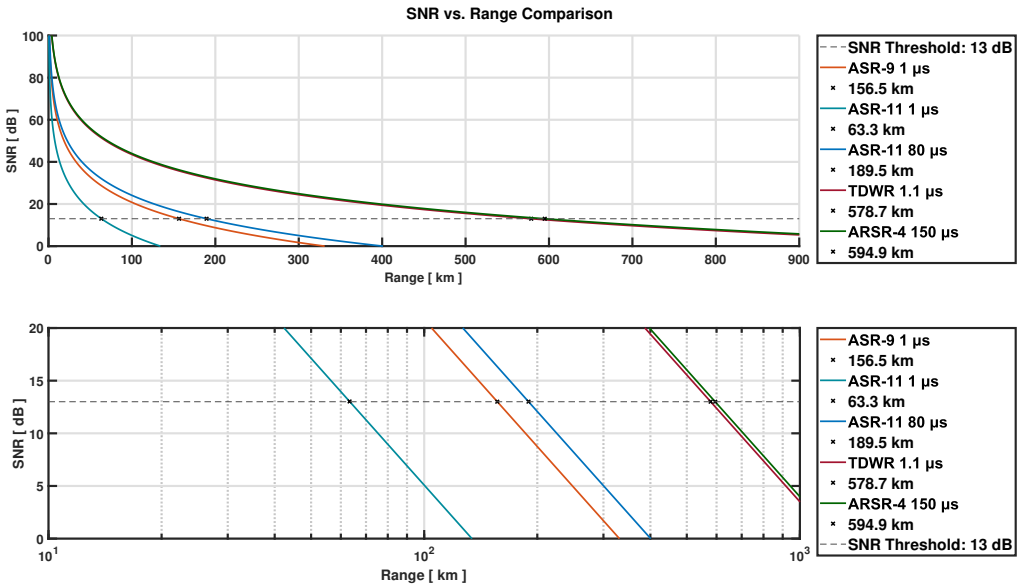

Figure 4.14. SNR vs. range with single pulse transmission for CN-235.

Performance curve order from the CN-235 is the same as the F-16, but with larger detection ranges. The larger aircraft RCS results in larger resulting detection range for all four radar systems. Of course, the benefits of the larger RCS value vary in positive effect as noted before. Comparing Figure 4.14 to the F-16 performance curves in Figure 4.1, the six-fold increase in RCS results in the following increases in detection range: 22.9 km for ASR-11 short pulse, 56.5 km for ASR-9, 68.5 km for ASR-11 long pulse, 209 km for TDWR, and 214.8 km for ARSR-4. Clearly, this marked increase in detection range across the radar systems will positively affect the TTA.

4.3.2 SNR vs. Range – Maximum Number of Pulses

This section considers the CN-235 using the same methodology as the F-16. Performance curves are shown in Figure 4.15.

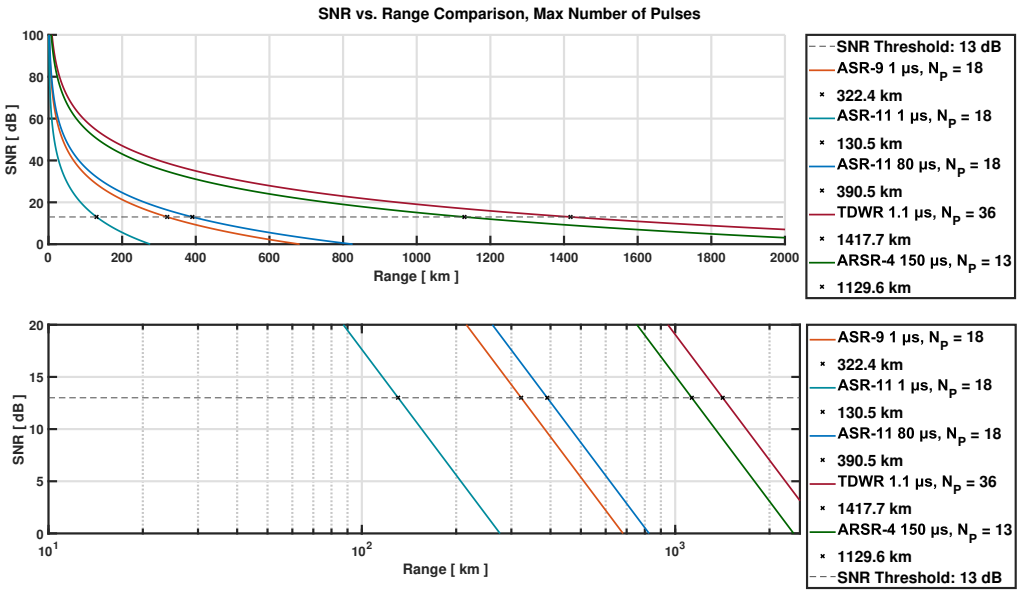

Figure 4.15. SNR vs. range with transmission of maximum number of pulses for CN-235.

Figure 4.15 order of radar performance curves matches Figure 4.2. The detection ranges in the maximum number of pulses comparison are quite large, especially for the ARSR-4 and TDWR. Increases in detection range over the F-16 with the maximum number of pulses are as follows: 47.2 km for ASR-11 short pulse, 116.4 km for ASR-9, 141 km for ASR-11 long pulse, 407.8 km for ARSR-4, and 511.9 km for TDWR.

4.3.3 Beam Comparison – Single Pulse

Figure 4.16 provides CN-235 performance curves for the radar system beams with center beam and HPBW detection ranges annotated.

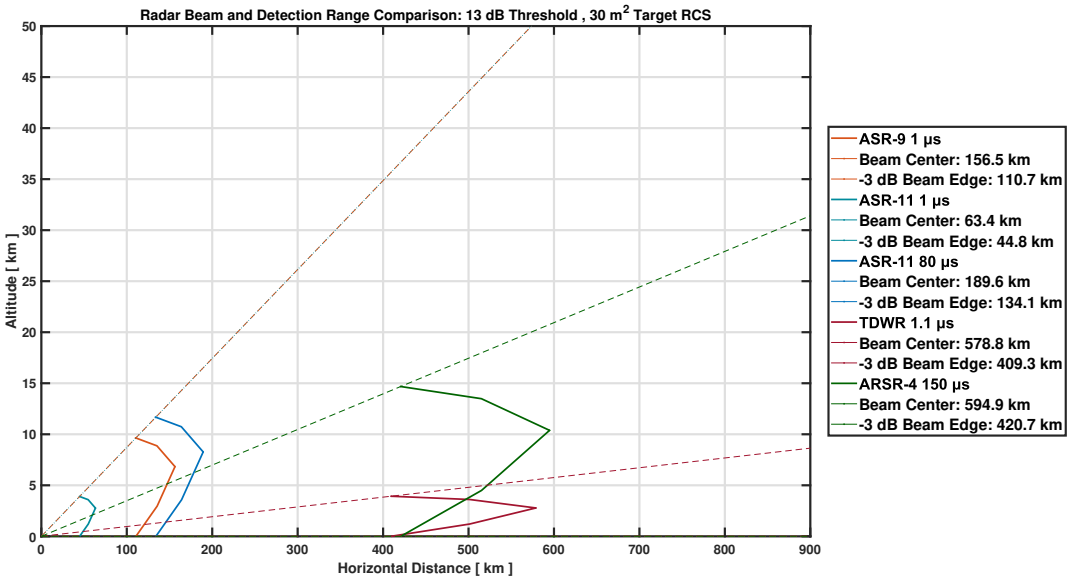

Figure 4.16. Radar beam comparison with single pulse transmission for CN-235.

The improved detection capability of the radar systems against a mid-size aircraft is clearly shown in Figure 4.16. The ARSR-4 provides the highest detection range. TTA values considering the CN-235 are as follows: 8.3 min for ASR-11 short pulse, 20.4 min for ASR-9, 24.7 min for ASR-11 long pulse, 75.5 min for TDWR, and 77.6 min for ARSR-4.

4.3.4 Beam Comparison – Maximum Number of Pulses

Figure 4.17 shows CN-235 performance curves with the maximum number of pulses.

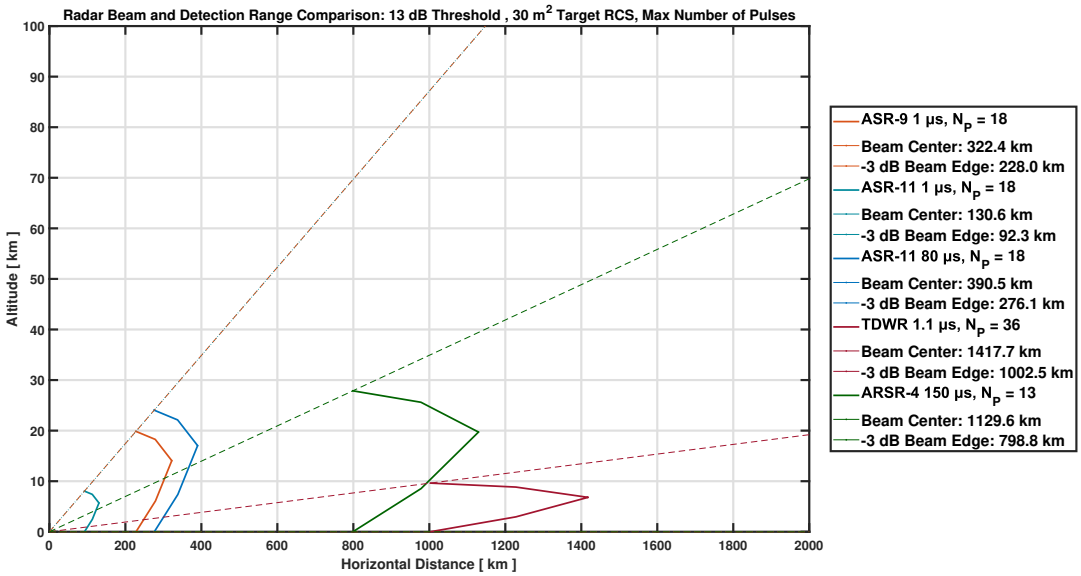

Figure 4.17. Radar beam comparison with transmission of maximum number of pulses for CN-235.

Figure 4.17 again confirms the order of radar performance seen in Figure 4.4. TTA values are as follows: 17 min for ASR-11 short pulse, 42.1 min for ASR-9, 51 min for ASR-11 long pulse, 147.4 min ARSR-4, and 185 min for TDWR. The detection range and TTA indicate a potential performance output given the assumptions and constraints.

4.3.5 Range vs. RCS – Single Pulse

Figure 4.18 shows radar performance curves related to target aircraft RCS. The RCS threshold is set to match the CN-235 RCS, while the detection SNR threshold remains at 13 dB.

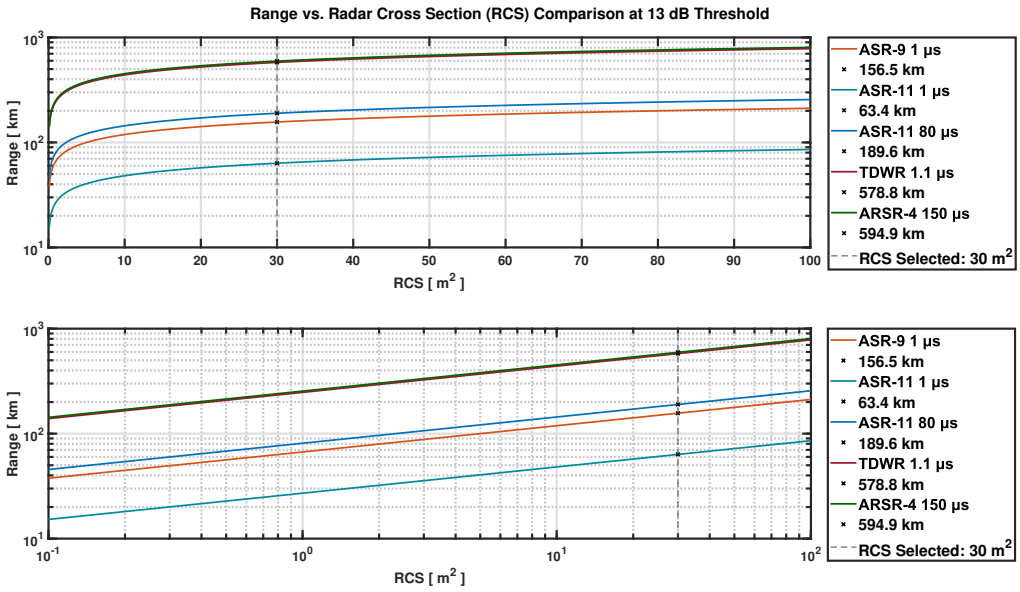

Figure 4.18. Range vs. RCS comparison with single pulse transmission for CN-235.

The ARSR-4 provides the largest detection range, and the ASR-11 short pulse provides the smallest. The detection range match the values from the SNR vs. range comparison for the CN-235 in Figure 4.16.

4.3.6 Range vs. RCS – Maximum Number of Pulses

Figure 4.19 depicts performance curves considering the maximum number of pulses. The TDWR shows the best performance using the maximum number of pulses. Recall that the TDWR increased detection range is at the expense of elevation beamwidth as the ARSR-4 provides higher elevation coverage at a shorter detection range and the opposite is true for the TDWR.

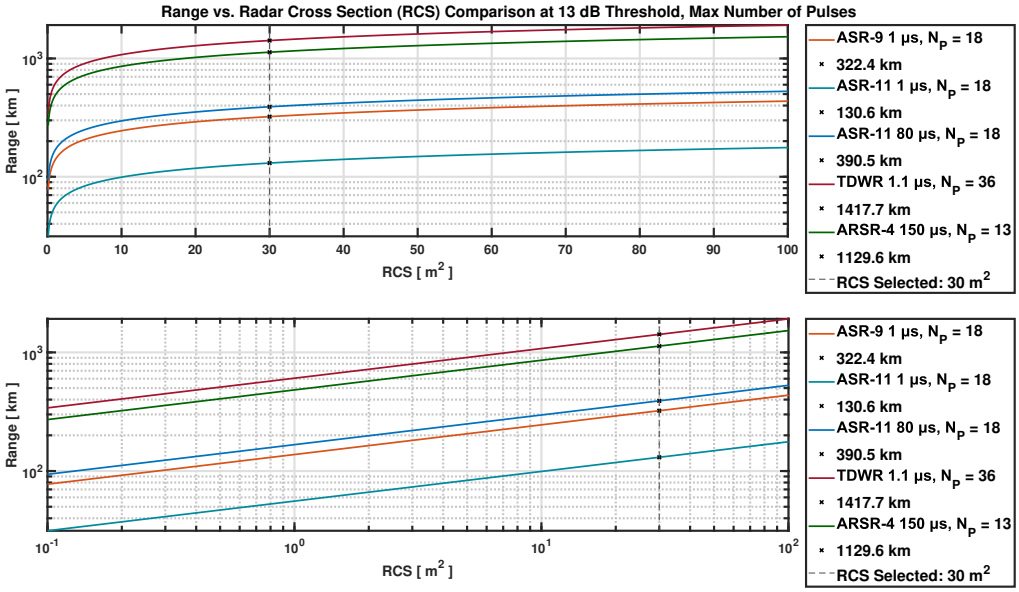

Figure 4.19. Range vs. RCS comparison with transmission of maximum number of pulses for CN-235.

4.3.7 Doppler Frequency Comparison

The Doppler frequency comparison uses the CN-235 maximum velocity of 127.7 m/s. This is much slower than the F-16, which travels at 408 m/s. One should anticipate a significant drop in Doppler frequency as Figure 4.20 confirms. While these Doppler frequencies are much lower, velocity aliasing occurs if the radar PRF (divided by 2) is lower than these Doppler values.

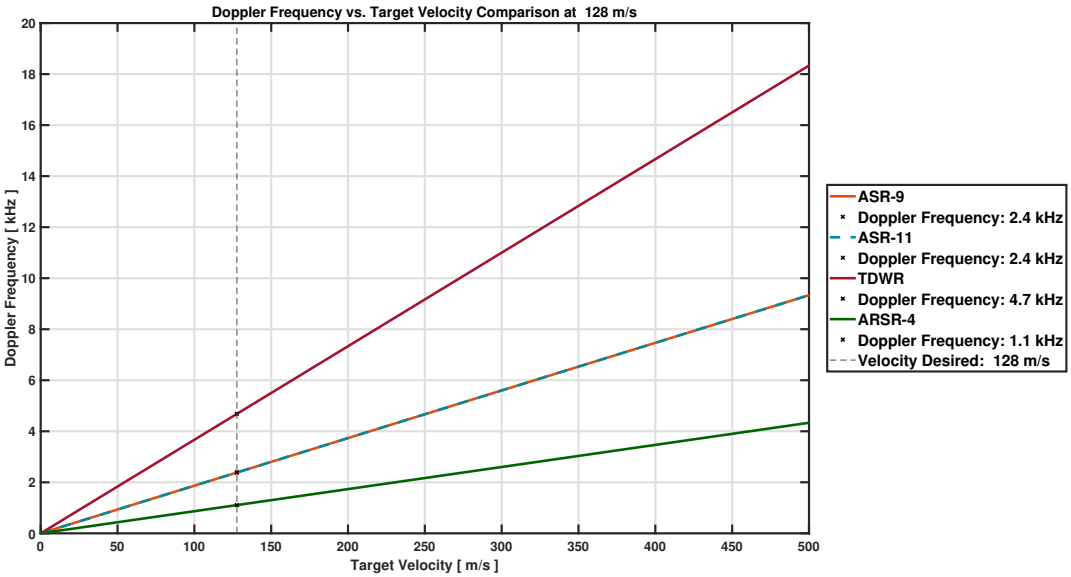

Figure 4.20. Doppler frequency vs. target velocity for CN-235.

4.4 CN-235 Summary

A noticeable improvement across all comparison metrics is evident as the CN-235 is a much larger and slower target than the F-16. Detection range and TTA are contained in Table 4.2.

Table 4.2. CN-235 summary of results.

CN-235	Units	ASR-9		ASR-11				TDWR		ARSR-4	
Pulse Width	us	1.0		1.0		80.0		1.1		150.0	
N_{Pulses}	-	Single	18	Single	18	Single	18	Single	36	Single	13
R_{max}	**km**	**156.5**	**322.4**	**63.4**	**130.6**	**189.6**	**390.5**	**578.8**	**1417.7**	**594.9**	**1129.6**
TTA_{max}	min	20.4	42.1	8.3	17.0	24.7	51.0	75.5	185.0	77.6	147.4
R_{-3dB}	**km**	**110.7**	**228.0**	**44.8**	**92.3**	**134.1**	**276.1**	**409.3**	**1002.5**	**420.7**	**798.8**
TTA_{-3dB}	min	14.4	29.8	5.9	12.1	17.5	36.0	53.4	130.8	54.9	104.3
$F_{doppler}$	kHz	2.4		2.4				4.7		1.1	
PRF	kHz	1.0		1.0				2.0		0.288	
Aliasing?	Y/N	Y		Y				Y		Y	

4.5 A310 Simulation Results

4.5.1 SNR vs. Range – Single Pulse

The final aircraft used in the comparison study is a large commercial aircraft with a high RCS. The A310 was at one time a popular aircraft for many commercial airlines around the world. The RCS and aircraft velocity values used are 100 m^2 and 272.2 m/s, respectively. Notably, this maximum velocity falls between the corresponding velocities of the CN-235 and the F-16. SNR vs. range performance set for single pulse transmission comparison is shown in Figure 4.21.

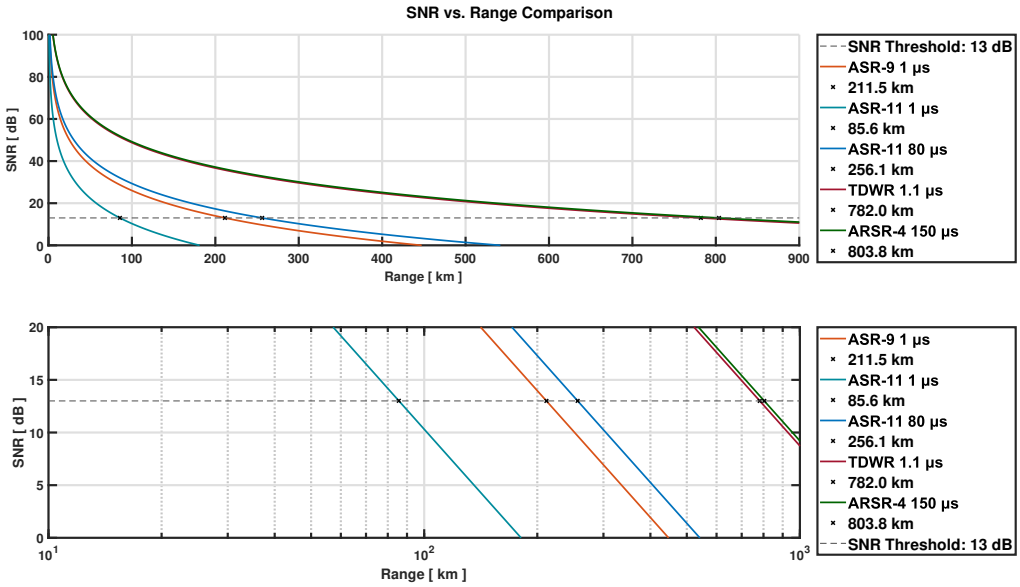

Figure 4.21. SNR vs. range with single pulse transmission for A310.

A310 performance curve order matches that of the F-16 and CN-235 but detection range is much larger. The increase of target aircraft RCS from 30 to 100 m^2 results in the following increases over the previous CN-235 performance set: 22.3 km for ASR-11 short pulse, 55 km for ASR-9, 66.6 km for ASR-11 long pulse, 203.3 km for TDWR, and 208.9 km for ARSR-4. Referring back to the CN-235 detection range increases over the F-16 in Section 4.3.1, it is interesting to note that the increase in RCS from 5 to 30 m^2 gives approximately

identical improvements in detection range as increasing from 30 to 100 m^2 in this case.

4.5.2 SNR vs. Range – Maximum Number of Pulses

Figure 4.22 shows performance results using the maximum number of pulses considering the A310.

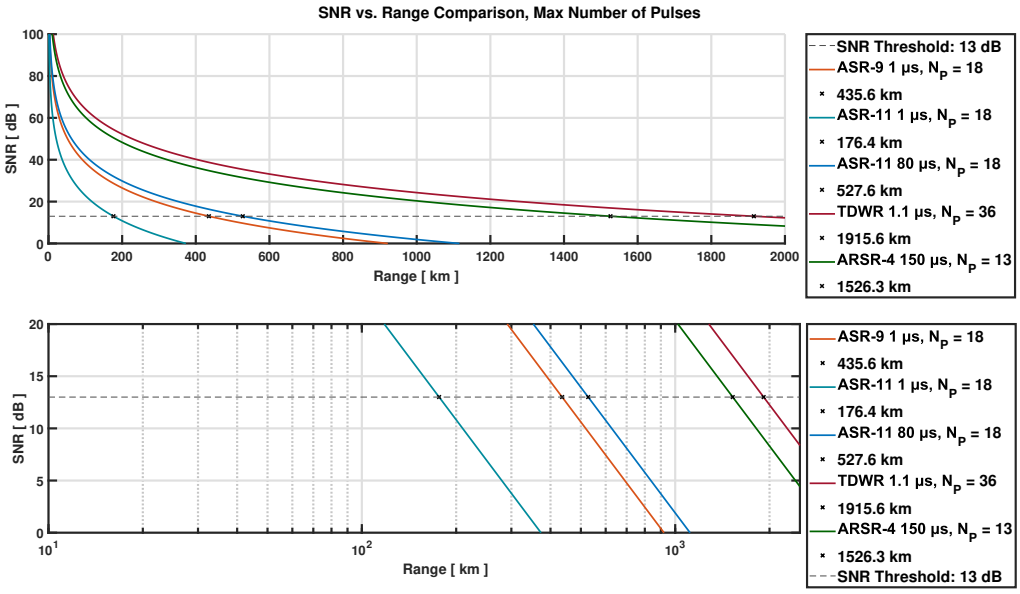

Figure 4.22. SNR vs. range with transmission of maximum number of pulses for A310.

It is clear how much the large RCS influences detection range, as the TDWR and ARSR-4 detection ranges go up to over 1000 km. Performance increase using the A310 over the CN-235 in the maximum number of pulses comparison are as follows: 45.8 km for ASR-11 short pulse, 113.3 km for ASR-9, 137.2 km for ASR-11 long pulse, 396.8 km for ARSR-4, and 497.9 km for TDWR.

4.5.3 Beam Comparison – Single Pulse

Figure 4.23 reports the radar beams and detection ranges for the A310 single pulse transmission.

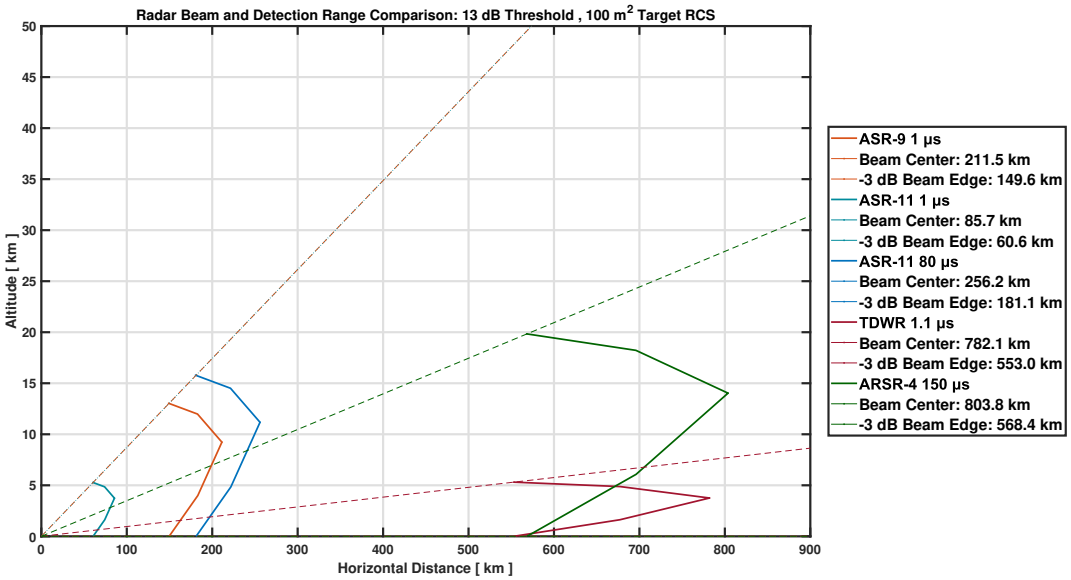

Figure 4.23. Radar beam comparison with single pulse transmission for A310.

The increase in detection ranges in Figure 4.23 have become significantly apparent, given the large size of the aircraft. Consistent with previous single pulse transmission results, the ARSR-4 indicates the highest detection range. TTA values for the radar systems are as follows: 5.2 min for ASR-11 short pulse, 13 min for ASR-9, 15.7 min for ASR-11 long pulse, 47.9 min for TDWR, and 49.2 min for ARSR-4. TTA is increased when compared to the CN-235 even though the A310 travels over twice as fast. This is due to increases in detection range for the larger RCS A310 outweighing the increase in aircraft speed from 127.7 m/s for the CN-235 to 272.2 m/s for the A310.

4.5.4 Beam Comparison – Maximum Number of Pulses

Figure 4.24 reports maximum number of pulses performance curves and detection ranges for the A310.

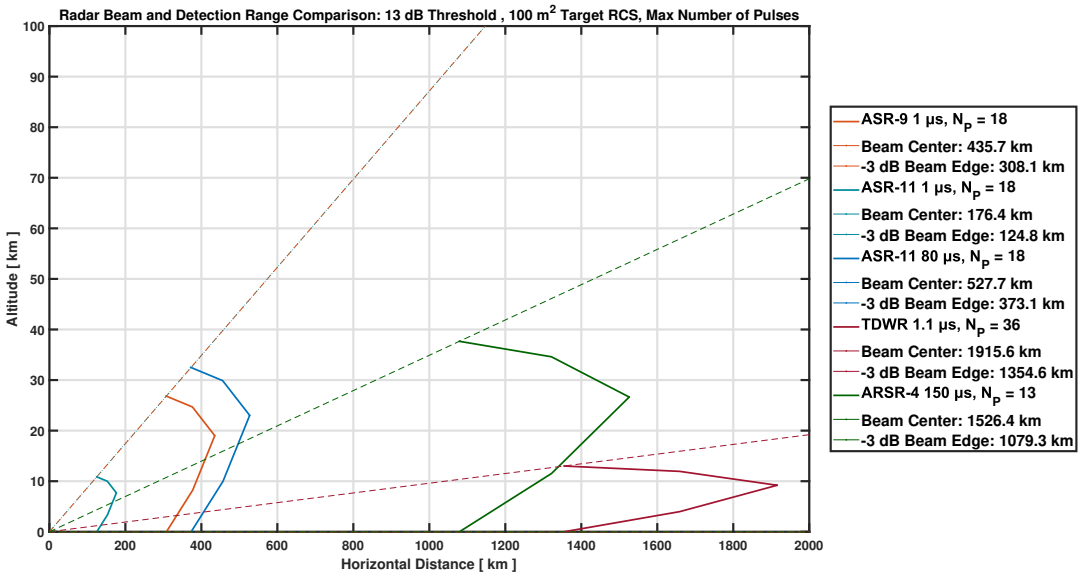

Figure 4.24. Radar beam comparison with transmission of maximum number of pulses for A310.

TDWR has the best performance with the maximum number of pulses considered. TTA values are as follows: 10.8 min for ASR-11 short pulse, 26.7 min for ASR-9, 32.3 min for ASR-11 long pulse, 93.5 min for ARSR-4, and 117.3 min for TDWR. As a reminder, detection range and TTA are very important output performance metrics given the assumptions and constraints.

4.5.5 Range vs. RCS – Single Pulse

Figure 4.25 reports detection range considering the target aircraft RCS. The RCS threshold used is the A310, RCS. Consistent with previous iterations, the detection threshold remains at 13 dB.

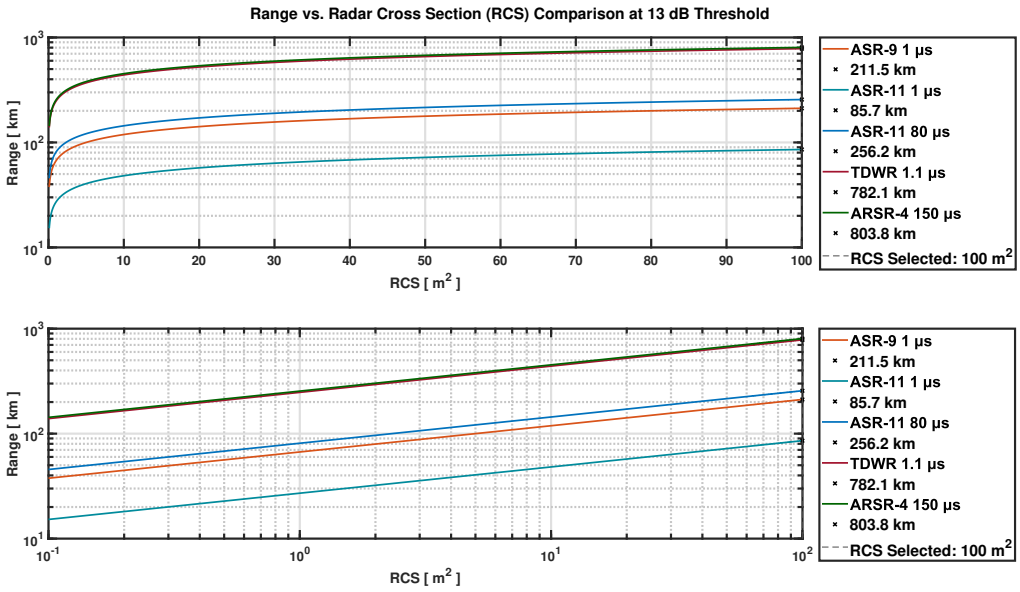

Figure 4.25. Range vs. RCS comparison with single pulse transmission for A310.

The A310 RCS coincides with the maximum RCS in the x-axis (100 m^2). In terms of the Matlab code set, a minor adjustment will accommodate for larger RCS aircraft such as a Boeing 747 or Airbus A380.

4.5.6 Range vs. RCS – Maximum Number of Pulses

Figure 4.26 reports the performance results considering the maximum number of pulses. Output detection range is consistent with SNR vs. range as indicated in Figure 4.22 with the TDWR reporting the highest detection range.

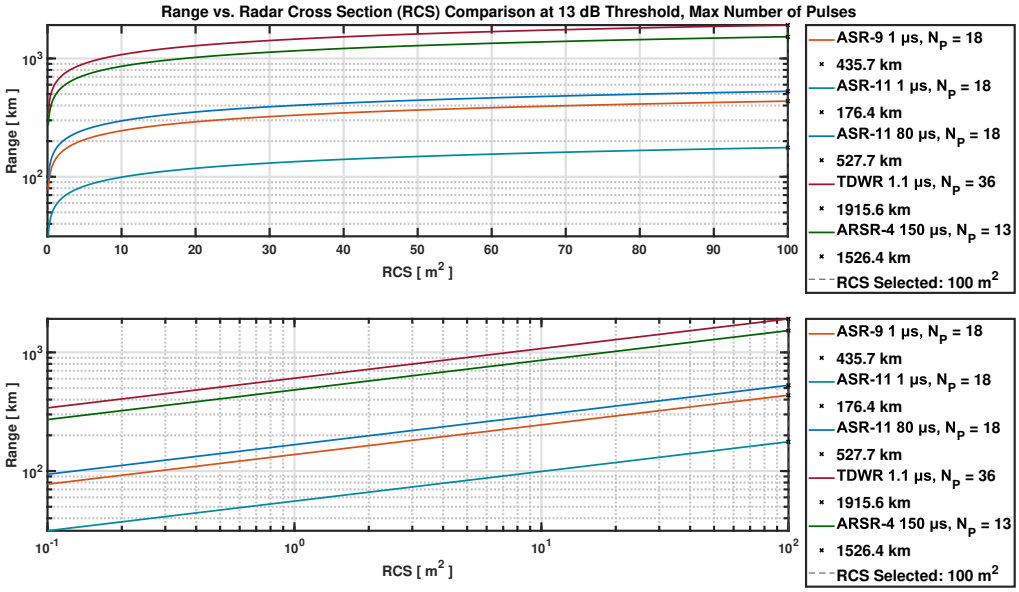

Figure 4.26. Range vs. RCS comparison with transmission of maximum number of pulses for A310.

4.5.7 Doppler Frequency Comparison

The A310 maximum velocity of 272.2 m/s falls between the CN-235 maximum velocity of 127.7 m/s and F-16 which travels at 408 m/s. Doppler frequency is reported in Figure 4.27. These Doppler frequencies listed in Figure 4.27 will induce aliasing at the receiver. It is noted that this amount of Doppler falls between the CN-235 and F-16 as expected.

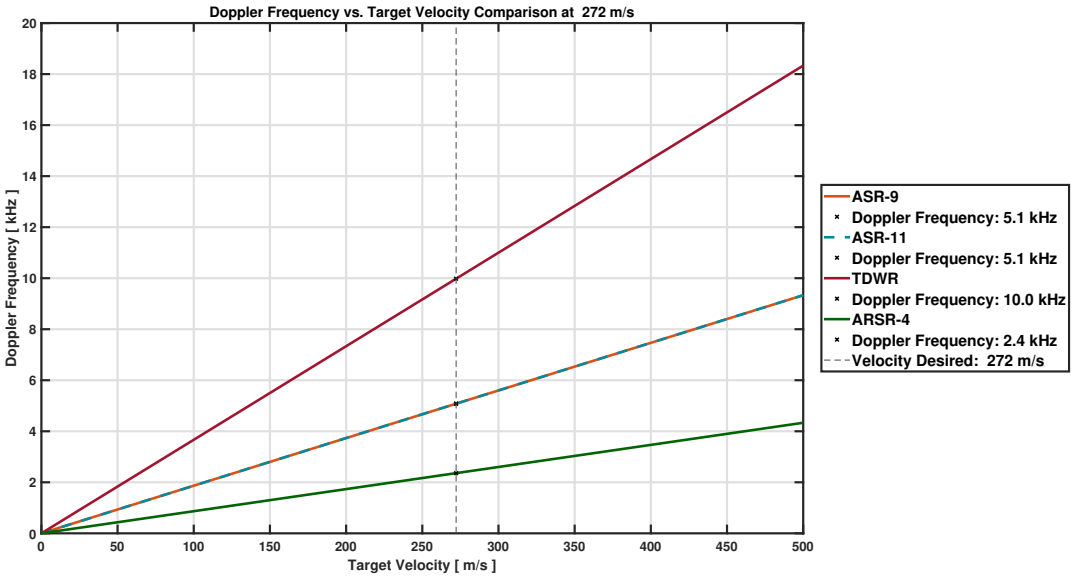

Figure 4.27. Doppler frequency vs. target velocity for A310.

4.6 A310 Summary

The A310 results in higher detection range and TTA values as compared to the CN-235. F-16 detection range and TTA are lower than the A310 in all categories except the Doppler frequency. Table 4.3 provides the final comparison summary considering the A310.

Table 4.3. A310 summary of results.

A310	Units	ASR-9		ASR-11				TDWR		ARSR-4	
Pulse Width	us	1.0		1.0		80.0		1.1		150.0	
N_{Pulses}	-	Single	18	Single	18	Single	18	Single	36	Single	13
R_{max}	**km**	**211.5**	**435.7**	**85.7**	**176.4**	**256.2**	**527.7**	**782.1**	**1915.6**	**803.8**	**1526.4**
TTA_{max}	min	13.0	26.7	5.2	10.8	15.7	32.3	47.9	117.3	49.2	93.5
R_{-3dB}	**km**	**149.6**	**308.1**	**60.6**	**124.8**	**181.1**	**373.1**	**553.0**	**1354.6**	**568.4**	**1079.3**
TTA_{-3dB}	min	9.2	18.9	3.7	7.6	11.1	22.8	33.9	82.9	34.8	66.1
$F_{doppler}$	kHz	5.1		5.1				10.0		2.4	
PRF	kHz	1.0		1.0				2.0		0.288	
Aliasing?	Y/N	Y		Y				Y		Y	

THIS PAGE INTENTIONALLY LEFT BLANK

CHAPTER 5:
Conclusion

5.1 Conclusion

In this work, we proposed to extend the capabilities of four FAA radars, namely the ASR-9, ASR-11, TDWR, and ARSR-4 allowing for the maximum number of pulses to be used in one antenna beamwidth. Moreover, coherent receiver processing is proposed that lowers the SNR required. A code set using Matlab was developed in support of research efforts. For comparison, SNR vs. range and range vs. RCS performance curves are generated for each radar corresponding to three aircraft, namely the F-16, CN-235, and A310. The TTA corresponding to maximum detection ranges are reported and Doppler frequency curves are generated. A special low-loss case of 3 dB utilizing the F-16 was considered and corresponding performance curves were generated.

Table 5.1 includes the radar systems, target aircraft, center beam and HPBW maximum theoretical detection ranges, and associated TTA values.

Table 5.1. Summary table of results. Includes all range values and TTA for center beam and HPBW.

Combined		Units	ASR-9		ASR-11				TDWR		ARSR-4	
Pulse Width		us	1.0		1.0		80.0		1.1		150.0	
N_{Pulses}		-	Single	18	Single	18	Single	18	Single	36	Single	13
F-16	R_{max}	km	**100.0**	**206.0**	**40.5**	**83.4**	**121.1**	**249.5**	**369.8**	**905.8**	**380.1**	**721.8**
	TTA_{max}	min	4.1	8.4	1.7	3.4	4.9	10.2	15.1	37.0	15.5	29.5
	R_{-3dB}	km	**70.7**	**145.7**	**28.6**	**59.0**	**85.7**	**176.4**	**261.5**	**640.5**	**268.8**	**510.4**
	TTA_{-3dB}	min	2.9	5.9	1.2	2.4	3.5	7.2	10.7	26.1	11.0	20.8
CN-235	R_{max}	km	**156.5**	**322.4**	**63.4**	**130.6**	**189.6**	**390.5**	**578.8**	**1417.7**	**594.9**	**1129.6**
	TTA_{max}	min	20.4	42.1	8.3	17.0	24.7	51.0	75.5	185.0	77.6	147.4
	R_{-3dB}	km	**110.7**	**228.0**	**44.8**	**92.3**	**134.1**	**276.1**	**409.3**	**1002.5**	**420.7**	**798.8**
	TTA_{-3dB}	min	14.4	29.8	5.9	12.1	17.5	36.0	53.4	130.8	54.9	104.3
A310	R_{max}	km	**211.5**	**435.7**	**85.7**	**176.4**	**256.2**	**527.7**	**782.1**	**1915.6**	**803.8**	**1526.4**
	TTA_{max}	min	13.0	26.7	5.2	10.8	15.7	32.3	47.9	117.3	49.2	93.5
	R_{-3dB}	km	**149.6**	**308.1**	**60.6**	**124.8**	**181.1**	**373.1**	**553.0**	**1354.6**	**568.4**	**1079.3**
	TTA_{-3dB}	min	9.2	18.9	3.7	7.6	11.1	22.8	33.9	82.9	34.8	66.1

Interesting findings include the similar performance between the ASR-9 and ASR-11 long pulse, even though there is a significant disparity in transmit power and pulse duration. It is clear that the updates to the ASR-11 radar have improved detection range performance over the older ASR-9 at a significantly lower peak power level. The ARSR-4 and TDWR also nearly have identical detection range with single pulse transmission. This is especially interesting since the radar parameters vary widely between the two systems. Additionally, performance curves corresponding to the maximum number of pulses produced different results for all cases considered compared to the performance curves with single pulse. As shown in Chapter 4, the TDWR detection range became larger than that of the ARSR-4 when the maximum number of pulses is used. This study produced a comprehensive set of performance capability for all four FAA radars if the maximum number of pulses and coherent receiver processing were to be used.

5.2 Future Work

There are opportunities for furthering this research. In terms of code improvements, increasing the automation associated with the code would be beneficial to provide performance results in a shorter time. This increased automation to the current code could be implemented through the use of a graphical interface for radar systems and target input parameters. The ability to rapidly change the number of radars (i.e., doing a side-by-side comparison of only two radars) being compared without altering the base code would prevent coding mistakes and ensure results are correct. That being said, this solution provides a solid foundation for more intricate comparisons and potential simulations.

For target alternatives and radar focused future work, there are many possibilities. The ability to determine radar performance relative to different aircraft sizes and velocities enables rapid comparisons to be made between results. Additionally, a multitude of scenario-based alterations to input parameters could be made. Ideas for scenarios include modifying power outputs for degraded operation, changing angle of aircraft approach, addition or reduction in losses associated with varying weather types and alternate radar system components, etc.

Finally, research into radar system design may also be fruitful with this existing research as a baseline, especially with the developed code set. One may develop a new radar design and quickly compare with the radars already programmed in the code.

THIS PAGE INTENTIONALLY LEFT BLANK

List of References

[1] Federal Aviation Administration, "Air traffic by the numbers." Accessed Jul. 1, 2023 [Online]. Available: https://www.faa.gov/air_traffic/by_the_numbers

[2] R. Doviak, M. Weber, and D. Zrnic, "Comparisons of weather and aircraft surveillance radar requirements to determine key features for a 10-cm multi-function phased array radar," in *2016 IEEE International Symposium on Phased Array Systems and Technology (PAST)*, 2016 [Online]. Available: http://ieeexplore.ieee.org/document/7832548/

[3] M. Weber, "FAA surveillance radar data as a complement to the WSR-88D network," in *Proc. Ninth Conf. on Aviation, Range, and Aerospace Meteorology and 20th Conf. on Severe Local Storms*, 2000 [Online]. Available: https://archive.ll.mit.edu/mission/aviation/publications/publication-files/ms-papers/Weber_2000_ARAM_MS-14191_WW-10147.pdf

[4] A. D. W. Sumari, A. I. Wuryandari, M. Darusman, and N. I. Utama, "The performance of supervised and unsupervised neural networks in performing aircraft identification tasks," in *Seminar Radar Nasional III 2009*, 2009 [Online]. Available: https://www.researchgate.net/publication/330370846_The_Performance_of_Supervised_and_Unsupervised_Neural_Networks_in_Performing_Aircraft_Identification_Tasks/link/5c3d1f10458515a4c726bac1/download

[5] M. Richards, J. Scheer, and W. Holm, *Principles of Modern Radar*. Raleigh, NC, USA: SciTech Pub, 2010.

[6] J. Kurdzo, "Pulse compression waveforms and applications for weather radar," Ph.D. dissertation, Sch. of Meteor., Univ. of Okl., Norman, OK, USA, 2015.

[7] J. V. Pieronek, "The ASR-9 processor augmentation card (9-PAC)," MIT Lincoln Lab, Lexington, MA, USA, Rep. ATC-232, 1995 [Online]. Available: https://archive.ll.mit.edu/mission/aviation/publications/publication-files/atc-reports/Pieronek_1995_ATC-232_WW-15318.pdf

[8] Kokolakis Contracting, "Tampa international airport, airport surveillance radar (ASR-9)." Accessed Jul. 3, 2023 [Online]. Available: https://www.jkokolakis.com/project/tia-airport-surveillance-radar-asr-9/

[9] M. Prata, "FAA technical center - Inside the fence," FAA. Accessed Jul. 3, 2023 [Online]. Available: https://www.tc.faa.gov/act4/insidethefence/2007/08_03_asr11.htm

[10] Federal Aviation Administration, "Airport surveillance radar (ASR-11)." Accessed Jul. 4, 2023 [Online]. Available: https://www.faa.gov/air_traffic/technology/asr-11

[11] Federal Aviation Administration, "Terminal doppler weather radar (TDWR)." Accessed Jul. 3, 2023 [Online]. Available: https://www.faa.gov/air_traffic/weather/tdwr

[12] Wikimapa, "Terminal doppler weather radar (TDWR) site." Accessed Jul. 3, 2023 [Online]. Available: http://wikimapia.org/31900572/Terminal-Doppler-Weather-Radar-TDWR-Site

[13] D. Henley, "84th RADES optimizes nation's LRR systems for air surveillance, national defense," 505th Command and Control Wing Public Affairs, USAF, Sep. 23, 2021 [Online]. Available: https://www.af.mil/News/Article-Display/Article/2786101/84th-rades-optimizes-nations-lrr-systems-for-air-surveillance-national-defense/https%3A%2F%2Fwww.af.mil%2FNews%2FArticle-Display%2FArticle%2F2786101%2F84th-rades-optimizes-nations-lrr-systems-for-air-surveillance-national-defense%2F

[14] F. Wiki, "ARSR-4 - fortwiki historic U.S. and canadian forts." Accessed Jul. 3, 2023 [Online]. Available: http://www.fortwiki.com/ARSR-4

[15] R. J. Lay, J. W. Taylor, and G. Brunins, "ARSR-4: unique solutions to long-recognized radar problems," in *IEEE International Conference on Radar*, 1990, pp. 6–11 [Online]. Available: https://ieeexplore.ieee.org/document/201129

[16] Statista Daily Data, "Infographic: The countries that use F-16 fighter jets." Accessed Jul. 3, 2023 [Online]. Available: https://www.statista.com/chart/30069/global-f16-fighter-jet-inventories

[17] US Air Force, "F-16 Fighting Falcon." Accessed Jul. 3, 2023 [Online]. Available: https://www.af.mil/About-Us/Fact-Sheets/Display/Article/104505/f-16-fighting-falcon/https%3A%2F%2Fwww.af.mil%2FAbout-Us%2FFact-Sheets%2FDisplay%2FArticle%2F104505%2Ff-16-fighting-falcon%2F

[18] Aviastar, "General Dynamics F-16." Accessed Jul. 1, 2023 [Online]. Available: http://aviastar.org/air/usa/general_f-16.php?p=1

[19] Airbus Military, "Airbus Military | CN235." Accessed Jul. 1, 2023 [Online]. Available: http://www.airbusmilitary.com/Aircraft/CN235/CN235Spec.aspx

[20] Military Factory, "Airbus Military (CASA) CN-235." Accessed Jul. 1, 2023 [Online]. Available: https://www.militaryfactory.com/aircraft/detail.php?aircraft_id=1018

[21] A. Industry, "Military aircrafts." Accessed Jul. 2, 2023 [Online]. Available: http://airbusindustry.podserver.info/military_aircrafts.html?i=1

[22] Airbus, "A310 Airbus." Accessed Jul. 5, 2023 [Online]. Available: https://www.airbus.com/en/who-we-are/our-history/commercial-aircraft-history/previous-generation-aircraft/a310

[23] N. Wenzel, "FedEx retires final Airbus A310 freighter," International Flight Network, Jan. 6, 2020 [Online]. Available: https://www.ifn.news/posts/fedex-retires-final-airbus-a310-freighter/

[24] C. Lofting, "Airbus A310-324 - Biman Bangladesh," Airliners.net, Jul. 7, 2007 [Online]. Available: https://www.airliners.net/photo/Biman-Bangladesh/Airbus-A310-324/1242729

[25] "Airbus A310," Dreams of Flying. Accessed Jul. 1, 2023 [Online]. Available: http://dreams-of-flying.blogspot.com/2010/07/airbus-a310.html

[26] National Telecommunications and Information Administration, "Automated measurement methods and technologies for the information society: A summary of an NTIA workshop," Boulder, CO, USA, Rep. 01-43, 2001 [Online]. Available: https://its.ntia.gov/umbraco/surface/download/publication?reportNumber=12-486.pdf

[27] S. S. Raymond, A. Abubakari, H. S. Jo, H. J. Hong, and H. K. Son, "Compatibility between LTE and airport surveillance radar in 2700–2900 MHz radar bands," in *2015 International Conference on Information and Communication Technology Convergence (ICTC)*, 2015 [Online]. Available: http://ieeexplore.ieee.org/document/7354732/

[28] J. E. Carroll, G. A. Sanders, F. H. Sanders, and R. L. Sole, "NTIA report TR-12-486 case study: Investigation of interference into 5 GHz weather radars from unlicensed national information infrastructure devices, part III," National Telecommunications and Information Administration, Boulder, CO, USA, Rep. TR-12-486, 2012 [Online]. Available: https://its.ntia.gov/umbraco/surface/download/publication?reportNumber=12-486.pdf

THIS PAGE INTENTIONALLY LEFT BLANK

Initial Distribution List

1. Defense Technical Information Center
   Ft. Belvoir, Virginia

2. Dudley Knox Library
   Naval Postgraduate School
   Monterey, California